Original Article

MOLECULAR METABOLISM

Reversal of diet-induced hepatic steatosis by peripheral CB1 receptor blockade in mice is p53/miRNA-22/SIRT1/PPARα dependent

Shahar Azar [1], Shiran Udi [1], Adi Drori [1], Rivka Hadar [1], Alina Nemirovski [1], Kiran V. Vemuri [2], Maya Miller [3], Dana Sherill-Rofe [3], Yhara Arad [3], Devorah Gur-Wahnon [4], Xiaoling Li [5], Alexandros Makriyannis [2], Danny Ben-Zvi [3], Yuval Tabach [3], Iddo Z. Ben-Dov [5], Joseph Tam [1,*]

ABSTRACT

Objective: The endocannabinoid (eCB) system is increasingly recognized as being crucially important in obesity-related hepatic steatosis. By activating the hepatic cannabinoid-1 receptor (CB_1R), eCBs modulate lipogenesis and fatty acid oxidation. However, the underlying molecular mechanisms are largely unknown.

Methods: We combined unbiased bioinformatics techniques, mouse genetic manipulations, multiple pharmacological, molecular, and cellular biology approaches, and genomic sequencing to systematically decipher the role of the hepatic CB_1R in modulating fat utilization in the liver and explored the downstream molecular mechanisms.

Results: Using an unbiased normalized phylogenetic profiling analysis, we found that the CB_1R evolutionarily coevolves with peroxisome proliferator-activated receptor-alpha (PPARα), a key regulator of hepatic lipid metabolism. In diet-induced obese (DIO) mice, peripheral CB_1R blockade (using AM6545) induced the reversal of hepatic steatosis and improved liver injury in WT, but not in PPARα$^{-/-}$ mice. The antisteatotic effect mediated by AM6545 in WT DIO mice was accompanied by increased hepatic expression and activity of PPARα as well as elevated hepatic levels of the PPARα-activating eCB-like molecules oleoylethanolamide and palmitoylethanolamide. Moreover, AM6545 was unable to rescue hepatic steatosis in DIO mice lacking liver sirtuin 1 (SIRT1), an upstream regulator of PPARα. Both of these signaling molecules were modulated by the CB_1R as measured in hepatocytes exposed to lipotoxic conditions or treated with CB_1R agonists in the absence/presence of AM6545. Furthermore, using microRNA transcriptomic profiling, we found that the CB_1R regulated the hepatic expression, acetylation, and transcriptional activity of p53, resulting in the enhanced expression of miR-22, which was found to specifically target SIRT1 and PPARα.

Conclusions: We provide strong evidence for a functional role of the p53/miR-22/SIRT1/PPARα signaling pathway in potentially mediating the antisteatotic effect of peripherally restricted CB_1R blockade.

Keywords Obesity; Fatty liver; Endocannabinoids; microRNAs; Nuclear receptor

1. INTRODUCTION

Non-alcoholic fatty liver disease (NAFLD) is the most common cause of chronic liver disease worldwide, affecting more than 25% of the human population, and a leading cause of morbidity and mortality [1]. NAFLD, considered the hepatic manifestation of metabolic syndrome, and its earliest stage, hepatic steatosis, are characterized by fat accumulation that exceeds 5% of hepatocytes in the absence of significant alcohol intake or secondary causes of lipid accumulation [1]. NAFLD is based on imbalances between lipid acquisition and removal that are regulated by *de novo* lipogenesis, fatty acid β-oxidation, uptake of circulating lipids, and their export to extrahepatic tissues. To date, various cellular, hormonal, metabolic, and genetic factors have been linked to its development [1], yet no effective medications have been approved to treat it.

Endocannabinoids (eCBs) are lipid ligands produced from membrane phospholipids; they activate the cannabinoid receptors to modulate food intake, body mass, and energy expenditure, mainly by activating the cannabinoid-1 receptor (CB_1R) abundantly expressed in the central nervous system and also present in peripheral tissues, such as the liver [2]. In fact, hepatic steatosis induced by a high-fat diet (HFD) depends on the activation of the peripheral CB_1Rs, including those in the liver. Global or hepatic nullification of the CB_1R protects mice from developing HFD-induced fatty liver [3,4]. Hepatocyte-selective

[1]Obesity and Metabolism Laboratory, Institute for Drug Research, School of Pharmacy, Faculty of Medicine, Hebrew University of Jerusalem, Jerusalem, Israel [2]Center for Drug Discovery, Northeastern University, Boston, MA, USA [3]Department of Developmental Biology and Cancer Research, Institute for Medical Research Israel-Canada, Hadassah Medical School, Hebrew University of Jerusalem, Jerusalem, Israel [4]Laboratory of Medical Transcriptomics, Department of Nephrology, Hadassah-Hebrew University Medical Center, Jerusalem, Israel [5]Laboratory of Signal Transduction, National Institute of Environmental Health Sciences, National Institutes of Health, Research Triangle Park, NC, USA

*__Corresponding author__. Joseph Tam, Obesity and Metabolism Laboratory, Institute for Drug Research, School of Pharmacy, Faculty of Medicine, P.O. Box 12065, Jerusalem, 9112001, Israel. Tel.: +972 2 675 7645; Fax: +972 2 675 7015. E-mail: yossi.tam@mail.huji.ac.il (J. Tam).

Received May 19, 2020 • Revision received September 3, 2020 • Accepted September 17, 2020 • Available online 26 September 2020

https://doi.org/10.1016/j.molmet.2020.101087

Abbreviations

2-AG	2-arachidonoylglycerol
AA	arachidonic acid
ACEA	arachidonyl-2′-chloroethylamide
AEA	anandamide/arachidonoylethanolamine
ALT	alanine aminotransferase
AST	aspartate aminotransferase
BAX	BCL-2-asocciated X apoptosis regulator
CB_1R	cannabinoid-1 receptor
CB_2R	cannabinoid-2 receptor
CBDA	cannabidiolic acid
CBG	cannabigerol
CBGA	cannabigerolic acid
DIO	diet-induced obesity
DOX	doxorubicin
eCB	endocannabinoid
FAAH	fatty acid amide hydrolase
FFA	free fatty acid
HFD	high-fat diet
LBD	ligand-binding domain
MAGL	monoacylglycerol lipase
miR	microRNA
NAD	nicotinamide adenine dinucleotide
NAFLD	non-alcoholic fatty liver disease
NASH	non-alcoholic steatohepatitis
NPP	normalized phylogenetic profiling
OEA	oleoylethanolamide
PCA	principal component analysis
PEA	palmitoylethanolamide
PFT-α	pifithrin-α
PPARα	peroxisome proliferator-activated receptor-alpha
PPRE	peroxisome proliferator response elements
PUMA	p53 upregulated modulator of apoptosis
SIRT1	sirtuin 1
THC	Δ^9-tetrahydrocannbidiol
Veh	vehicle
WT	wild-type

overexpression of the CB_1R in mice increases the accumulation of triglycerides in the liver, although these mice are resistant to diet-induced obesity (DIO) [5,6]. Likewise, pharmacological blockade of the CB_1R by globally acting or peripherally restricted CB_1R antagonists improves hepatic steatosis in mice [6–8] and humans [9] by reducing lipogenic gene expression [3,6,8] and upregulating fatty acid β-oxidation [4,6,8,10]. However, to date, the specific molecular mechanism by which CB_1R activation/blockade contributes to the development/reversal of NAFLD remains elusive.

2. MATERIALS AND METHODS

2.1. Normalized phylogenetic profiling

To generate the normalized phylogenetic profiling (NPP) data [11–14], proteomes of 1,029 species, including humans, were downloaded from UniProt (June 2018 release) [15]. Short proteins with lengths of fewer than 40 amino acids were excluded. When multiple isoforms were annotated for the same gene, we retained only the longest isoform. Species were annotated according to the NCBI Taxonomy Database [16]. NPP was based on the similarity between the query (human) protein and the best hit BLAST measure [17,18] in each of the different species. To reduce noise, bitscores smaller than threshold t were clipped ("floored") to t, where $t = 20.4$. This bitscore threshold was the minimal bitscore value across all of the species that corresponded to an E value less than or equal to 0.05.

Each of the best BLAST hit's bitscores was first normalized by the bitscore of the query protein self-hit [19]. Then, the log2 of the normalized bitscore was calculated. The log scores were normalized by the level of conservation for all of the proteins in the specific proteome by Z scoring all of the scores for a specific species [13,14]. Thus, we based our global analysis on a $\sim$20,000 genes $\times$ $\sim$1000 species NPP matrix, in which each data point $x_{a,b}$ was the NPP score for gene a in species b compared to that of humans. Based on the resulting NPP matrix, we constructed a $\sim$20,000 $\times$ 20,000 correlation matrix containing the Pearson correlation coefficients between the phylogenetic profiles of every gene pair.

2.2. Animals and experimental protocol

The experimental protocol used was approved by the Institutional Animal Care and Use Committee of Hebrew University (AAALAC accreditation #1285), reported in compliance with the ARRIVE guidelines [20], and based on the principles of replacement, refinement, and reduction. Male six-week-old liver-specific CB_1R null mice ($LCB1^{-/-}$) [4], $PPAR\alpha^{-/-}$ (kindly provided to us by Jeffrey M. Peters of Pennsylvania State University) [21], and liver-specific $SIRT1^{-/-}$ ($LSIRT1^{-/-}$) [22] mice and their littermate C57Bl/6 controls were housed under specific pathogen-free (SPF) conditions up to five per cage in standard plastic cages with natural soft sawdust as bedding. The animals were maintained under a controlled temperature of 22–24 °C at 55 $\pm$ 5% humidity and alternating 12-h light/dark cycles (lights were on between 7:00 and 19:00); the animals were provided food and water *ad libitum*. To generate DIO, the mice were fed a HFD (Research Diet; D12492; 60% of Kcal from fat, 20% from protein, and 20% from carbohydrates) for 14 weeks. Then HFD-fed wild-type, $PPAR\alpha^{-/-}$, or $LSIRT1^{-/-}$ obese mice received either vehicle (Veh; 1% Tween80, 4% DMSO, and 95% saline) or the peripherally restricted CB_1R antagonist AM6545 (10 mg/kg) daily for 7 days by intraperitoneal injections. Body weight and food intake were monitored daily. The mice were euthanized by cervical dislocation, their livers were removed and either snap-frozen or fixed in buffered 4% formalin, and trunk blood was collected to determine endocrine and biochemical parameters.

2.3. Glucose tolerance (ipGTT) and insulin sensitivity tests (ipIST)

Mice that were fasted overnight were injected with glucose (1.5 g/kg i.p.), followed by tail blood collection at 0, 15, 30, 45, 60, 90, and 120 min. Blood glucose levels were determined using an Elite glucometer (Bayer, Pittsburgh, PA, USA). On the following day, the mice were fasted for 6 h before receiving insulin (0.75 U/kg, i.p.; Eli Lilly, Indianapolis, IN, USA, or Actrapid vials, Novo Nordisk A/S, Bagsværd, Denmark) and blood glucose levels were determined at the same intervals as previously described.

2.4. Blood chemistry

Serum alanine aminotransferase (ALT) and aspartate aminotransferase (AST) were quantified using AMS Vegasys (Diamond Diagnostics, Holliston, MA, USA) or Cobas C-111 Chemistry Analyzers (Roche, Basel, Switzerland). Blood glucose was determined using an Elite glucometer (Bayer). Serum insulin was determined using an Ultra-Sensitive Mouse Insulin ELISA kit (Crystal Chem Inc., Elk Grove

Village, IL, USA or Millipore, Darmstadt, Germany). Serum leptin and adiponectin were determined by ELISA (B-Bridge International, Santa Clara, CA, USA).

2.5. Hepatic triglyceride content

Liver tissue was extracted as previously described [23] and its triglyceride content was determined using an EnzyChrom Triglyceride assay kit (BioAssay Systems, Hayward, CA, USA).

2.6. Cell culture

HepG2 cells (ATCC HB-8065) or immortalized mouse primary hepatocytes described in [24] were cultured in RPMI-1640 media (Biological Industries, Beit HaEmek, Israel) containing 10% Fetal Bovine Serum (FBS; Cat# 12657, Gibco Biosciences, Dublin, Ireland) at 37 °C in a humidified atmosphere of 5% CO_2/95% air. Cell experiments were conducted at > 80% confluence in 6-well plates (7.5×10^5 cells/well) as follows:

2.6.1. CB_1R agonism/antagonism treatment

Cells were cultured in a serum-free RPMI-1640 medium for 16 h. The peripherally restricted CB_1R antagonist AM6545 was then added to the medium at a final concentration of 1 μM, and 1 h later, the cells were exposed to arachidonyl-2′-chloroethylamide (ACEA; Cat# 91054, Cayman Chemical, Ann Arbor, MI, USA) at final concentrations of 1–10 μM or to HU-210 at a final concentration of 100 nM for 24 h.

2.6.2. CB_2R agonism treatment

Cells were cultured in a serum-free RPMI-1640 medium for 16 h. The cells were then exposed to HU-308 at a final concentration of 100 nM for 24 h.

2.6.3. FAAH and MAGL inhibition

Cells were cultured in a serum-free RPMI-1640 medium for 16 h. The dual FAAH and MAGL inhibitor JZL195 was then added to the medium at a final concentration of 250 nM for 24 h.

2.6.4. Lipotoxic conditions

Cells were cultured in RPMI-1640 containing 1% fatty acid-free bovine serum albumin (BSA; Cat# A7030; Sigma–Aldrich, St. Louis, MO, USA). AM6545 was added to the medium at a final concentration of 1 μM, followed by the addition of a mixed solution of sodium oleate (Cat# 07501; Sigma–Aldrich) and sodium palmitate (Cat# P9767; Sigma–Aldrich) at a ratio of 2:1, respectively, at a final concentration of 0.3–1 mM.

2.6.5. Transcriptional inhibition of p53

Cells were cultured in a serum-free RPMI-1640 medium for 16 h. Then pifithrin-α (PFT-α; Cat# 16209; Cayman Chemical) was added to the medium at a final concentration of 25 μM, followed by the addition of JZL195 at a final concentration of 250 nM for an additional 24 h.

2.6.6. p53 activation

Cells were cultured in a serum-free RPMI-1640 medium for 16 h. Then doxorubicin (DOX) was added to the medium at a final concentration of 1.9 μM for 24 h.

2.7. Mimic-miR-22–3p and antago-miR-22–3p transfection

HepG2 cells were transfected with miRIDIAN microRNA hsa-miR-22–3p mimic (Cat# C-300493-03; Dharmacon, Lafayette, CO, USA) or miRIDIAN microRNA hsa-miR-22–3p hairpin inhibitor (Cat# C-300493-05; Dharmacon) using lipofectamine 3000 (Cat# L3000-001; Invitrogen, Carlsbad, CA, USA), according to the manufacturer's protocol.

2.8. Luciferase reporter assay

2.8.1. PPARα activity assay

To measure PPARα activity, HepG2 cells were seeded in 96-well plates and transfected with PPRE X3-TK-luc and pRL-SV40P plasmids (Cat# 1015 and 27163, respectively; Addgene, Watertown, MA, USA) at a ratio of 1:40 using lipofectamine 3000 (Cat# L3000-001; Invitrogen), according to the manufacturer's protocol. Transfected cells were treated with ACEA at a final concentration of 10 μM for 24 h. Luciferase activity was measured using a Dual-Glo Luciferase assay system (Cat# E2920; Promega, Madison, WI, USA) according to the manufacturer's protocol.

2.8.2. miR-22 direct target assay

To determine whether PPARα and SIRT1 are direct targets of miR-22, HepG2 cells were seeded in 96-well plates and co-transfected with miRIDIAN microRNA hsa-miR-22–3p mimic (Cat# C-300493-03; Dharmacon) with a custom-made plasmid containing the luciferase reporter gene paired to the PPARα 3′UTR sequence (Cat# CS-HmiT105045-MT06-02; Genecopoeia, Rockville, MD, USA) or the SIRT1 3′UTR miRNA Reporter LeniVector (Cat# 438060810195; Applied Biological Materials, Richmond, BC, Canada) and a pRL-SV40P plasmid (Cat# 27163; Addgene) at a ratio of 1:40 using lipofectamine 3000 (Cat# L3000-001; Invitrogen) according to the manufacturer's protocol. After 16 h, the luciferase activity was measured using a Dual-Glo Luciferase assay system (Cat# E2920; Promega) according to the manufacturer's protocol.

2.9. p53 transcriptional activity assay

HepG2 cells were incubated in black 96-well plates (Cat# 655090; Greiner, Kremsmünster, Austria) at a density of 4×10^5 cells per well. After 24 h, the cells were transfected with pGF-p53-mCMV-EF1α-Puro lentivector (Cat# TR200PA-P; System Biosciences, Palo Alto, CA, USA) using lipofectamine 3000 (Cat# L3000-001; Invitrogen) according to the manufacturer's protocol. After 8 h, the transfected cells were treated with ACEA at a final concentration of 10 μM or DOX at a final concentration of 1.9 μM for 24 h. The medium from each well was replaced by 1x PBS, and the fluorescence intensity was measured with a SpectraMax iD3 microplate reader (Molecular Devices, San Jose, CA, USA) at a wavelength of ex:470/em:510 nm for GFP. The results were normalized to the total protein levels in each well.

2.10. Cellular fat accumulation

HepG2 cells were incubated in black 96-well plates (Cat# 655090; Greiner) at a density of 4×10^5 cells per well and treated with O:P (2:1, respectively) at final concentrations of 0.3–1 mM for 24 h. Each well was washed twice with 1x PBS and then stained with Nile Red (Cat# 19123; Sigma–Aldrich) and Hoechst by adding a Nile Red/Hoechst mixed solution (1 μg/mL; diluted in 1x PBS) to the cells for 15 min at 37 °C. The cells were then washed with 1x PBS, and the fluorescence intensity was measured with a SpectraMax iD3 microplate reader (Molecular Devices) at wavelengths of ex:488/em:550 and ex:350/em:461 nm for Nile Red and Hoechst, respectively. The results were normalized to the total protein levels of each well and presented as a change in the accumulation of lipids in comparison with the Veh-treated group.

2.11. Western blotting

Liver homogenates were prepared in a RIPA buffer (Thermo Fisher Scientific, Rockford, IL, USA; 25 mM Tris–HCl pH 7.6, 150 mM NaCl, 1% NP-40, 1% sodium deoxycholate, and 0.1% SDS) using

BulletBlender and zirconium oxide beads (Next Advanced, Inc., Troy, NY, USA). Cells were harvested and precipitated in 1x PBS and then resuspended in RIPA buffer. Protein concentrations were measured with a Pierce BCA Protein assay kit (Thermo Fisher Scientific). Samples were resolved by SDS-PAGE (4–15% acrylamide, 150V) and transferred to PVDF or nitrocellulose membranes using a Trans-Blot Turbo Transfer System (Bio-Rad, Hercules, CA, USA). Membranes were then incubated for 1 h in 5% milk (in 1xTBS-T) to block unspecific binding. Blots were incubated overnight with primary antibodies against PPARα (1:1000; Cat# ab8934, Abcam Cambridge, MA, USA), SIRT1 (1:1000; Cat# 9475S, Cell Signaling Technology, Danvers, MA, USA), P53(1C12) (1:500; Cat# 2524, Cell Signaling Technology), and Ac-P53 (Lys382) (1:750; Cat# 2525, Cell Signaling Technology) at 4 °C or with β-actin horseradish peroxidase (HRP)-conjugated primary antibody (1:30000; Cat# ab49900, Abcam) for 1 h at room temperature. Anti-rabbit (1:2500; Cat# ab97085, Abcam) or anti-mouse (1:5000; Cat# ab98799, Abcam) HRP-conjugated secondary antibodies were used for 1 h at room temperature, followed by chemiluminescence detection using a Clarity Western ECL Blotting Substrate (Bio-Rad). Densitometry was quantified using ImageJ and Image Lab software.

2.12. Nuclear localization of p53

Cells were harvested and precipitated in 1x PBS. Their nuclear fraction was extracted using a Nuclear Extraction kit (Cat# ab113474, Abcam) according to the manufacturer's protocol, and the expression levels of p53 were measured by Western blotting against fibrillarin (1:750; Cat# ab4566, Abcam).

2.13. Real-time PCR

Total RNA from mouse livers and HepG2 cells was extracted using TRIzol (Invitrogen), followed by DNase I treatment (Invitrogen), and reverse-transcribed using an Iscript cDNA kit (Bio-Rad). Real-time PCR was conducted using iTaq Universal SYBR Green Supermix (Bio-Rad) and the CFX connect ST system (Bio-Rad). The human and mouse primer list is detailed in Supplementary Table 5. Normalization was performed against human or mouse *β-actin* and *Gapdh*. Pri-miR-22 expression was measured by real-time PCR on cDNA synthesized from total RNA, which was isolated as previously described.

MiRNA from total RNA extracted from mouse livers and HepG2 cells was purified using TRIzol, followed by an overnight ethanol precipitation. cDNA was synthesized using a qScript microRNA cDNA Synthesis kit (Cat# 95107; Quanta Biosciences, Beverly, MA, USA). MicroRNA expression was measured by real-time PCR using PerfeCTa SYBR Green Supermix (Cat# 95054; Quanta Biosciences). Normalization of miR-22–3p (PerfeCTa microRNA assay) was performed against human or mouse RNU6 (PerfeCTa microRNA assay). Total RNA was also used for in-house small RNA library preparation and miRNA sequence profiling as previously described [25]. The resulting FASTQ files were demultiplexed, mapped, and annotated using a published pipeline [26].

2.14. Histopathology

Five μm paraffin-embedded liver sections were stained with hematoxylin and eosin staining. Liver images were captured with a Zeiss AxioCam ICc5 color camera mounted on a Zeiss Axio Scope A1 light microscope and taken from 10 random 40x fields for each animal. Lipid staining was conducted using an Oil Red O staining kit (Cat# ab150678; Abcam) according to the manufacturer's protocol. Briefly, 20 μm optimal cutting temperature (O.C.T) (4583; SciGen, Inc., Gardena, CA, USA) compound-embedded liver sections were placed in propylene glycerol, followed by an Oil Red O solution and hematoxylin staining. Stained sections were photographed as previously described.

2.15. Immunohistochemistry

Liver tissues were fixed in buffered 4% formalin for 48 h and then embedded in paraffin. Sections were deparaffinized and hydrated. Heat-mediated antigen retrieval was performed with 10 mM citrate buffer pH 6.0 (Thermo Fisher Scientific). Endogenous peroxide was inhibited by incubating with a freshly prepared 3% H_2O_2 solution in MeOH. Unspecific antigens were blocked by incubating sections for 1 h with 2.5% horse serum (Cat# VE-S-2000; Vector Laboratories, Burlingame, CA, USA). To assess the PPARα expression, 5 μm liver sections were stained with rabbit anti-mouse PPARα (1:400; Cat# ab61182; Abcam), followed by a goat anti-rabbit or HRP conjugate (ImmPRESS; Vector Laboratories). Color was developed after incubation with 3,3′-diaminobenzidine (DAB) substrate (Cat# SK-4105; Vector Laboratories; ImmPACT DAB Peroxidase (HRP) substrate), followed by hematoxylin counterstaining and mounting (Cat# Vecmount H-5000; Vector Laboratories). Stained sections were photographed as previously described. The positive area was quantified using ImageJ with a minimum of 5–6 random liver sections per mouse.

2.16. FAAH and MAGL activity

The ability of AM6545 to modulate fatty acid amide hydrolase (FAAH) and monoacylglycerol lipase (MAGL) activity was tested using inhibitor screening kits (Cayman Chemical) based on the release of a fluorophore from a synthetic substrate by recombinant human FAAH and MAGL.

2.17. Endocannabinoid measurements

The extraction, purification, and quantification of anandamide (AEA), 2-arachydonoylglycerol (2-AG), arachidonic acid (AA), oleoylethanolamide (OEA), and palmitoylethanolamide (PEA) in mouse liver tissue were performed by stable isotope dilution liquid chromatography/tandem mass spectrometry (LC-MS/MS) as previously described [27].

2.18. SIRT1 activity assay

Mouse livers were homogenated in a lysis buffer (Cat# ab152163; Abcam) using BulletBlender and zirconium oxide beads (Next Advanced). SIRT1 immunoprecipitation and activity assays were conducted according to the manufacturer's protocol (Cat# ab156065; Abcam). Briefly, a SIRT1 primary antibody (Cat# 2028; Cell Signaling Technology) was incubated overnight with liver lysates at 4 °C. Samples were then incubated with protein A/G PLUS-Agarose (Cat# sc-2003; Santa Cruz Biotechnology, Heidelberg, Germany) and precipitated by centrifugation. After three washes with a lysis buffer, the purified SIRT1 reconstituted with the reaction mix and was loaded into 96-well plates (Cat# 655090; Greiner). The fluorescence intensity was measured with a SpectraMax iD3 reader (Molecular Devices) at a wavelength of ex:340/em:460 nm.

2.19. Time-resolved fluorescence resonance energy transfer (TR-FRET) assays *in vitro*

To measure ligand binding to PPARα, TR-FRET was performed with a LanthaScreen TR-FRET PPARα competitive binding assay according to the manufacturer's instructions (Invitrogen). Briefly, a serial dilution of AM6545 and GW7647, a selective PPARα agonist, was prepared in a 384-well polypropylene assay plate. Fluormone Pan-PPAR Green, PPARα-LBD, and terbium (Tb)-labeled anti-GST Abs were then added to each sample. The assay plate was incubated for 2 h at room temperature prior to measuring the 520 nm/495 nm emission ratio of each well using an Infinite F500 microplate reader (Tecan, Männedorf, Switzerland) with instrument settings as described in the manufacturer's instructions for LanthaScreen assays.

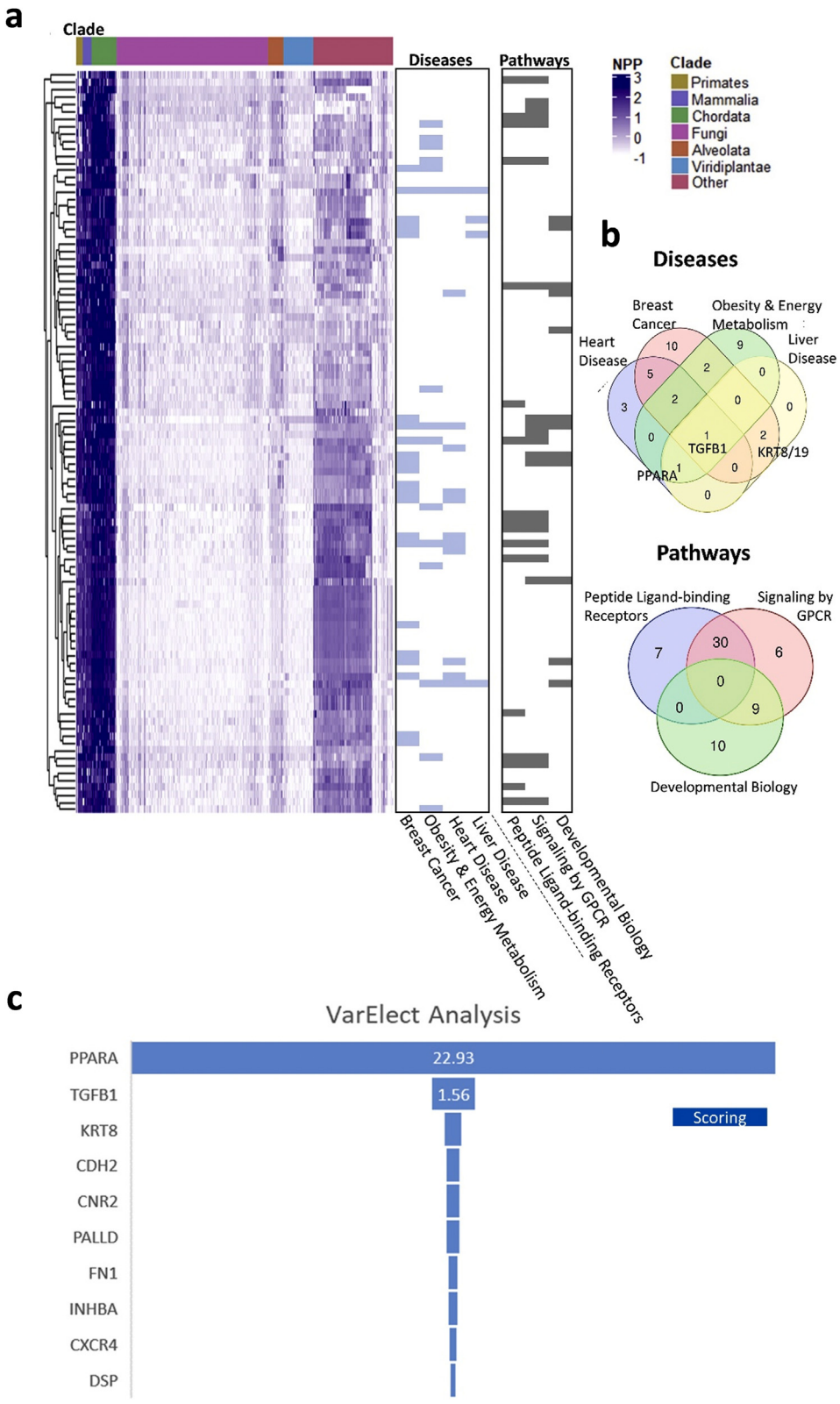

Figure 1: Analysis of phylogenetic profiling of the top 100 coevolved genes related to *CNR1*. (A) A normalized phylogenetic profile (NPP) gene by species; each row represents the NPP of a single gene across 1,028 species (columns) ordered by their phylogenetic distance from *Homo sapiens*. The colors in the heat map indicate the relative degree of conservation between human protein and its ortholog in a certain species (column). The bars on the right side represent genes enriched for (i) diseases: breast cancer, obesity and energy metabolism, heart disease and liver disease, or (ii) pathways: peptide ligand-binding receptors, signaling by GPCR, and developmental biology. (B) Venn diagrams representing the intersecting genes between the tested disease/pathway-associated genes analyzed with GeneAnalytics. *TGFB1*, *PPARA*, *KRT8*, and *KRT19* are among the most representative genes within the tested diseases. (C) VarElect analysis ranking genes to phenotype/diseases terms. Applied on the top 100 coevolved genes with *CNR1* annotated to NAFLD, revealing *PPARA* to be the top ranked gene.

2.20. PPARα reporter assay

Activation of PPARα was quantified by a human PPARα reporter assay (Indigo Biosciences, State College, PA, USA) according to the manufacturer's instructions. Briefly, overexpressed PPARα reporter cells were dispensed into a 96-well plate, then immediately dosed with AM6545 and/or synthetic agonist GW590735. Following 22 h of incubation, the treatment media were discarded and luciferase detection reagent was added. The light emission intensity from the ensuing luciferase reaction was quantified after 15 min using a BioTek Synergy 2 luminometer; it was directly proportional to the relative level of PPARα activation in the reporter cells. DMSO levels were equal in all of the samples and never exceeded 0.1%. The results are reported as the percent activation compared to DMSO-only controls.

2.21. Materials

AM6545 was synthesized at the Center for Drug Discovery, Northeastern University, Boston, MA, USA. ACEA (Cat# 91054), PFT-α (Cat# 16209), and JZL195 (Cat# 13668) were purchased from Cayman Chemical. HU-210 and HU-308 were kindly provided by Prof. Raphael Mechoulam of Hebrew University, Jerusalem, Israel. DOX was kindly provided by Prof. Yinon Ben Neriah of Hebrew University, Jerusalem, Israel.

2.22. Human analysis

Human transcriptomics data were reanalyzed from the GSE48452 and GSE106737 data sets (Gene Expression Omnibus repository accession numbers) that were published in Ahrens et al. 2013 [28] and Haas et al. 2019 [29], respectively. Data were quantile normalized and transcripts were filtered by a threshold value to attain normal distribution.

2.23. Statistics

Values are expressed as the mean ± SEM. Unpaired two-tailed Student's t-test was used to determine differences between the Veh- and drug-treated groups. The results in multiple groups and time-dependent variables were compared by ANOVA, followed by a Bonferroni test (GraphPad Prism v6 for Windows). Significance was at $P < 0.05$. Deep sequencing-based miRNA count profiles were analyzed using the DESeq2 [30] and edgeR [31] R/Bioconductor statistical packages as previously described [25].

3. RESULTS

3.1. Hepatic CB_1R regulates PPARα expression and activity

To impartially identify proteins that are functionally linked to the CB_1R and that may contribute to its role in modulating fat utilization in the liver, we employed NPP analysis [14] of the CB_1R gene (*CNR1*) to detect genes that locally coevolved with it and are functionally related as previously demonstrated [13]. Our analysis revealed the top 100 genes (53 genes remained after paralog filtration) that coevolved with the CB_1R (Figure 1A and Supplementary Table 1). In agreement with *CNR1* being an eCB receptor protein, applying GeneAnalytics [32] analysis and performing enrichment for diseases and pathways revealed that these genes are generally related to proteins involved in breast cancer, obesity and energy metabolism, heart and liver diseases, as well as peptide-ligand binding receptors and signaling by GPCR (Figure 1A,B and Supplementary Table 2). Intersecting the obtained gene sets revealed a handful of genes: *TGFB1*, *PPARA*, *KRT8*, and *KRT19*. To further identify which of the CB_1R coevolved genes are also associated with NAFLD, we applied the VarElect tool [32], generating rank-ordered NAFLD-related prioritization on the top 100 *CNR1* coevolved genes. The top-ranked gene was peroxisome proliferator-activated receptor-alpha (PPARα; $P < 0.0002$, Figure 1C), which is abundantly expressed in the liver and an important modulator of hepatic lipid metabolism. Upon activation, PPARα is known to stimulate the transcription of target genes by binding to peroxisome proliferator response elements (PPRE), resulting in the activation of mitochondrial and peroxisomal fatty acid β-oxidation pathways as well as lipid uptake and transport [33]. Its genetic deletion predisposes mice to develop hepatic steatosis and steatohepatitis [34,35], whereas its activation protects the liver from DIO-induced NAFLD [34] and inflammation [35].

To assess whether hepatic PPARα is directly modulated by the CB_1R, we checked its expression levels in hepatocytes following specific pharmacological modulation of the CB_1R. Stimulating the CB_1R using ACEA downregulated the mRNA and protein levels of PPARα (Figure 2A–C) as well as its activity as manifested by reducing the promoter activity of PPRE using a Luciferase reporter assay (Figure 2D) and downregulating the expression of its targeted genes (Figure 2E). These effects were significantly reversed by pretreating the cells with the peripherally restricted CB_1R antagonist AM6545. Both a 7-day treatment of WT DIO mice with AM6545 and hepatocyte ablation of the CB_1R in the DIO mice resulted in the induction of the hepatic expression of PPARα (Figure 2F–K), an effect that triggered a significant upregulation of its targeted genes *in vivo* (Figure 2L and M). To exclude the possibility that AM6545 binds to the ligand-binding domain (LBD) of PPARα and directly or allosterically activates it, three *in vitro* assays were performed: a TR-FRET-based competitive ligand-binding assay, a PPARα functional activity assay, and an allosteric modulation assessment of PPARα. Compared with the selective PPARα agonists GW7647 and GW590735, AM6545 failed to either bind to or act on PPARα directly/allosterically (Supplementary Fig. 1). Taken together, these findings suggest that hepatic PPARα is controlled by the CB_1R.

3.2. Peripheral CB_1R blockade attenuates hepatic steatosis via PPARα

We next examined the metabolic effect of AM6545 in WT and PPARα$^{-/-}$ mice fed a HFD for 14 weeks. A significant reduction in body weight and hepatic steatosis was evident as early as after 7 days of treating DIO mice with AM6545 (10 mg/kg, i.p.) [6]. In agreement with previous reports [34,35], both wild-type and PPARα$^{-/-}$ mice became obese on a HFD; however, treatment with AM6545 significantly reduced their body weight (Supplementary Fig. 2a). While an insignificant reduction was measured in fasting blood glucose levels (Supplementary Fig. 2b), short-term AM6545 treatment significantly reduced hyperinsulinemia (Supplementary Fig. 2c) and glucose intolerance (Supplementary Figs. 2d and e) without affecting insulin sensitivity (Supplementary Figs. 2f and g) in both the WT and PPARα$^{-/-}$ DIO mice. Both AM6545-treated genotypes exhibited reduced hyperleptinemia (Supplementary Fig. 2h) and elevated adiponectin levels (Supplementary Fig. 2i). Surprisingly, the HFD-induced hepatic steatosis as manifested by elevated fat accumulation in the liver, increased hepatic triglyceride content, and hepatocellular damage, manifested by elevated circulating ALT and AST levels, was significantly reduced by AM6545 in DIO WT, but not in the obese PPARα$^{-/-}$ mice (Figure 3A–D). Moreover, AM6545 failed to increase the expression of PPARα-related genes in the null mice (Figure 3E and Figure 2L). These findings suggest a PPARα-dependent mechanism by which peripheral CB_1R blockade attenuates DIO-related fatty liver.

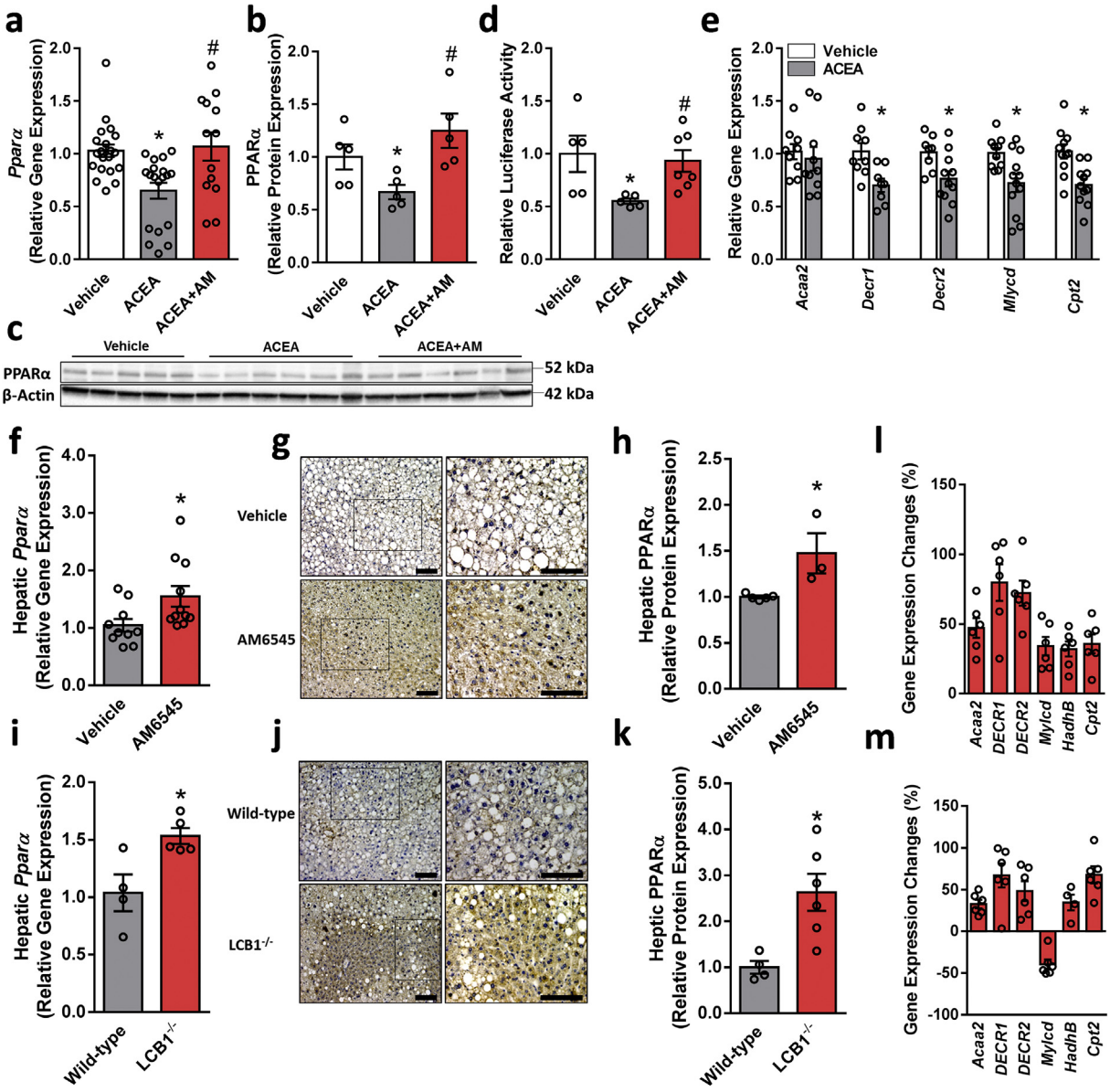

Figure 2: CB_1R regulates PPARα expression and activity. Changes in the mRNA (A) and protein (B and C) expression as well as activity (D) of PPARα in hepatocytes exposed to vehicle or ACEA (10 μM) in the absence/presence of AM6545 (1 μM) for 24 h. ACEA reduced the mRNA expression levels of PPARα-related target genes in hepatocytes (E). Male six-week-old C57Bl/6 and $LCB1^{-/-}$ mice were fed a HFD for 14 weeks. Then C57Bl/6 mice were treated with AM6545 (10 mg/kg, i.p.) for 7 days. Increased mRNA (F and I) and protein (G, H, J, and K) expression of hepatic PPARα was found in AM6545-treated and obese $LCB1^{-/-}$ mice. The relative expression levels of PPARα-related target genes in the livers of obese WT treated with AM6545 (L) or $LCB1^{-/-}$ (M). The values represent the percent fold change in expression relative to vehicle-treated animals (L) or WT littermate controls (M). *In vitro* data represent the mean ± SEM from 2 to 5 independent experiments. $^{*}P < 0.05$ relative to vehicle-treated cells. $^{\#}P < 0.05$ relative to ACEA-treated cells. *In vivo* data represent the mean ± SEM from 5 to 11 mice per group. $^{*}P < 0.05$ relative to vehicle-treated or wild-type groups. For panels G and J, original magnification of ×20 and × 40. Scale bars, 100 μm.

3.3. Pharmacological blockade or genetic deletion of CB_1R elevates the hepatic levels of eCB-like molecules

PPARα is a ligand activated by endogenous agonists, which include free fatty acids (FFAs) and their derivatives, such as eCBs. In fact, several lines of evidence suggest that a link exists between the eCB system and PPARα. For instance, selected cannabinoids and their analogs (such as 15-HETE-G, OEA, PEA, AEA, and WIN-55,212−2) are PPARα agonists [36−41]. Therefore, we next assessed the endogenous hepatic levels of eCBs and their analogs in DIO mice treated with AM6545. We found that although 2-AG levels did not change significantly (Supplementary Figs. 3a), a robust upregulation in the hepatic levels of AEA, AA, OEA, and PEA was measured following peripheral CB_1R blockade (Supplementary Figs. 3b−e). This suggests a link between the blockade of CB_1R and the increased hepatic activation of PPARα caused by its endogenous occurring ligands. Although the AM6545-induced elevation in the AEA levels might contribute to the activation of the CB_1R to enhance hepatic *de novo* lipogenesis [3], the present findings support an opposite mechanism whereby the eCB-like molecules OEA and PEA contribute to the activation of PPARα, resulting in increased FFA β-oxidation. Similar observations were also found in mice lacking the CB_1R specifically in hepatocytes (Supplementary Figs. 3f−j). The elevated OEA and PEA levels following the blockade

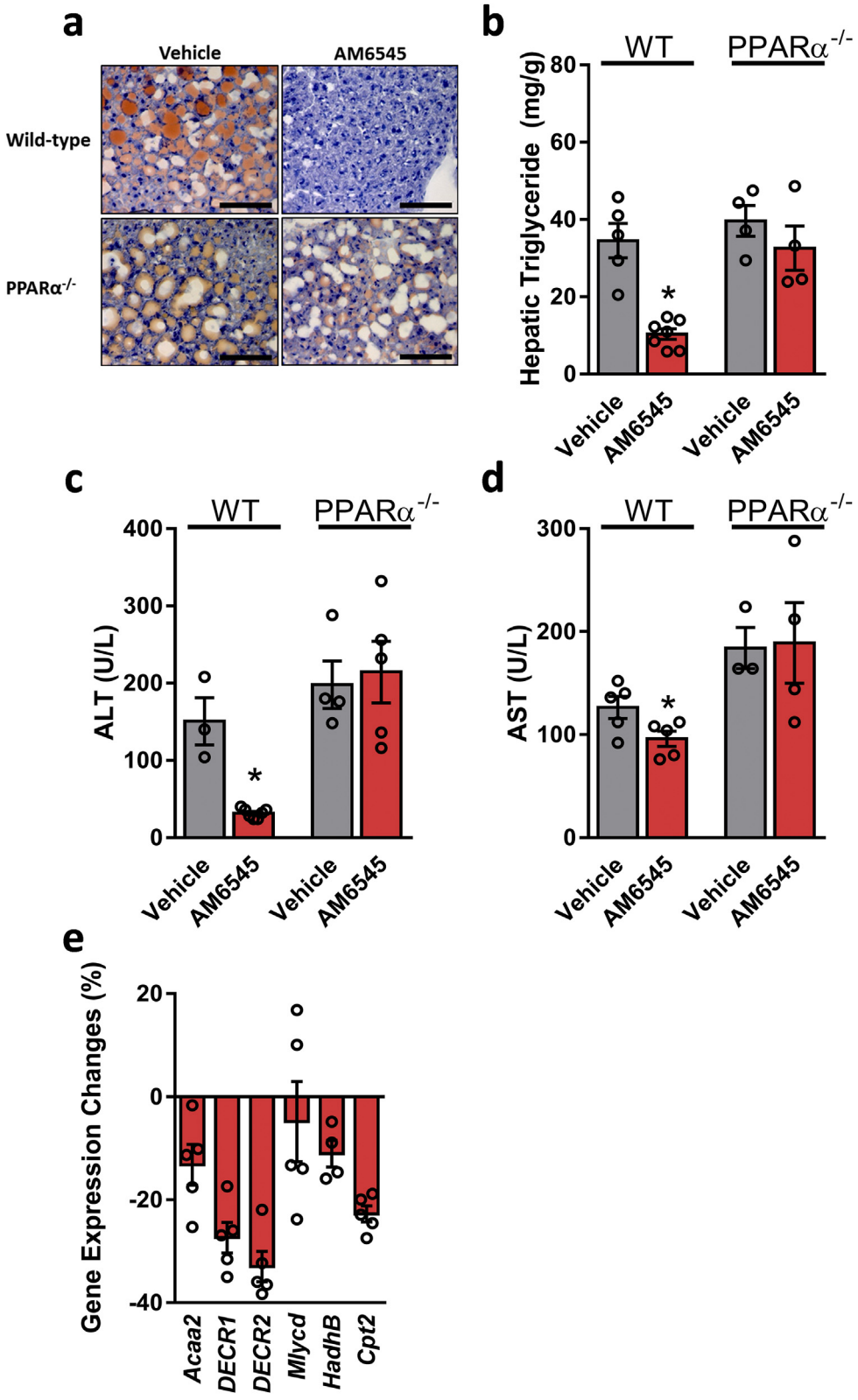

Figure 3: Reversal of HFD-induced hepatic steatosis and hepatic injury by peripheral CB_1R blockade is PPARα dependent. Male six-week-old PPARα$^{-/-}$ and their littermate control mice were fed a HFD for 14 weeks and then treated with AM6545 (10 mg/kg, i.p.) for 7 days. AM6545 failed to reverse HFD-induced hepatic steatosis in PPARα$^{-/-}$ mice as documented by Oil Red O staining of liver sections (A), hepatic triglyceride quantification (B), and serum ALT (C) and AST (D) levels. The relative expression levels of PPARα-related target genes in the livers of PPARα$^{-/-}$ mice treated with AM6545 (E). The values represent the percent fold change in expression relative to the WT littermate controls. Data represent the mean ± SEM from 4 to 7 mice per group. *$P < 0.05$ relative to the vehicle-treated group from the same strain. For panel A, original magnification of × 40. Scale bars, 100 μm.

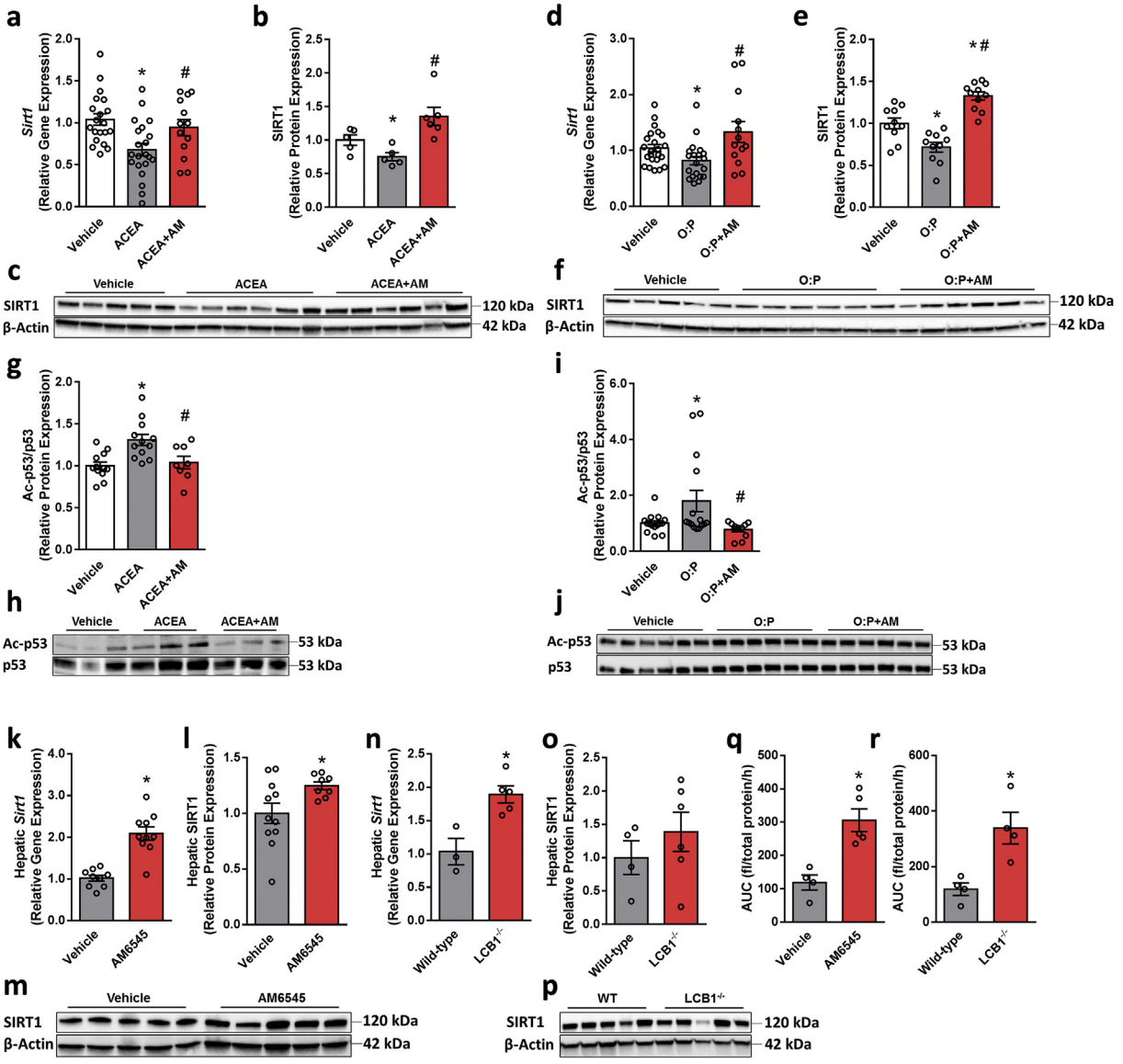

Figure 4: CB_1R regulates SIRT1 expression and activity. Changes in the mRNA (A and D) and protein (B, C, E, and F) expression of SIRT1 in hepatocytes exposed to vehicle, ACEA (10 μM), or a 1 mM mixture of oleate and palmitate (O:P = 2:1, respectively) in the absence/presence of AM6545 (1 μM) for 24 h. *In vitro* SIRT1 activity (G–J) was assessed by monitoring the acetylation levels of p53, which was inhibited by ACEA and O:P and increased following pretreatment of the cells with AM6545. *In vivo* hepatic SIRT1 expression and activity were measured in male six-week-old C57Bl/6 and $LCB1^{-/-}$ mice fed a HFD for 14 weeks. Wild-type mice were treated with AM6545 (10 mg/kg, i.p.) for 7 days. Increased mRNA (K and N) and protein (L, M, O, and P) expression of hepatic SIRT1 was documented in AM6545-treated and $LCB1^{-/-}$ mice. AM6545 increased SIRT1 activity as measured using a SIRT1 activity assay in liver homogenates from WT DIO mice treated with AM6545 or obese $LCB1^{-/-}$ animals (Q, R). *In vitro* data represent the mean ± SEM from 3 to 5 independent experiments. $^{*}P < 0.05$ relative to vehicle-treated cells. $^{\#}P < 0.05$ relative to ACEA- or O:P-treated cells. *In vivo* data represent the mean ± SEM from 5 to 12 mice per group. $^{*}P < 0.05$ relative to the vehicle-treated or wild-type groups.

of the CB_1R by AM6545 was probably related to their increased synthesis rather than the direct inhibition of their breakdown, since AM6545 was not found to affect FAAH or MAGL activity (Supplementary Fig. 3k and l).

3.4. Hepatic CB_1R regulates SIRT1 expression and activity

Recent evidence indicates that inhibiting the hepatic function of NAD^{+}-dependent histone deacetylase sirtuin 1 (SIRT1), a key modulator of hepatic PPARα activity, contributes to DIO-related hepatic steatosis [22], whereas SIRT1 activation protects against DIO-induced metabolic disorders by increasing fatty acid β-oxidation [42]. In fact, liver-specific SIRT1 knockout ($LSIRT1^{-/-}$) mice display impaired hepatic PPARα signaling, which is accompanied by enhanced hepatic fat accumulation when challenged with a HFD [22]. Therefore, we next evaluated whether the expression and function of SIRT1 are also regulated by the CB_1R. Similar to its effect on PPARα, CB_1R activation or lipotoxicity reduced the expression and deacetylase activity of SIRT1 in hepatocytes, whereas blocking the CB_1R by AM6545 normalized these changes (Figure 4A–J). Moreover, elevated hepatic levels of SIRT1 were found in both the WT DIO mice treated with AM6545 (Figure 4K–M) and obese liver-specific CB_1R null animals (Figure 4N–P), an increase that resulted in enhanced activity (Figure 4Q and R), suggesting that hepatic SIRT1 is also regulated by the CB_1R.

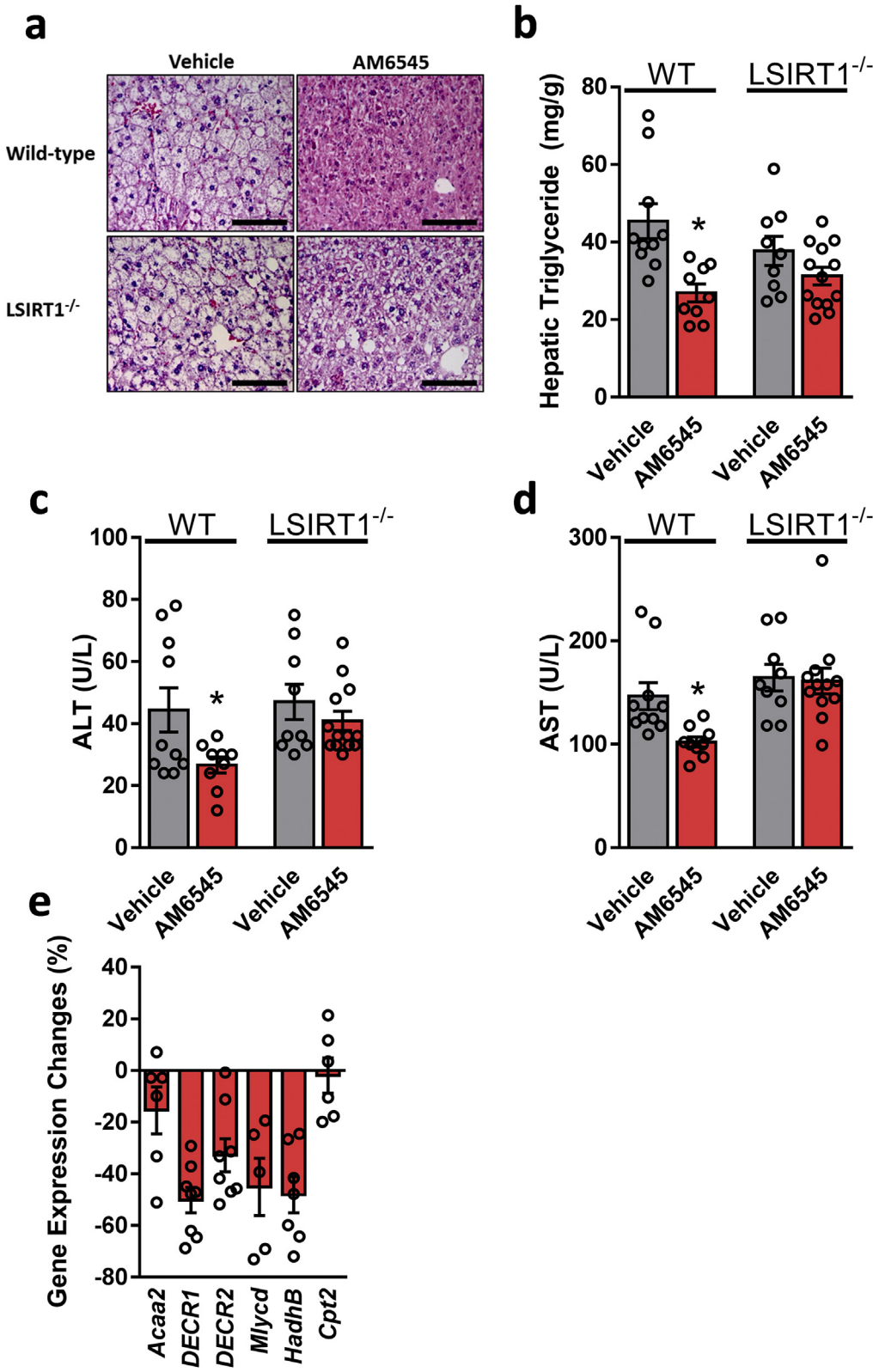

Figure 5: Reversal of HFD-induced hepatic steatosis and hepatic injury by peripheral CB_1R blockade is SIRT1 dependent. Male six-week-old LSIRT1$^{-/-}$ and their littermate control mice were fed a HFD for 14 weeks and then treated with AM6545 (10 mg/kg, i.p.) for 7 days. AM6545 failed to reverse HFD-induced hepatic steatosis in LSIRT1$^{-/-}$ mice as manifested by fat accumulation in hepatocytes (A), hepatic triglyceride quantification (B), and elevated serum ALT (C) and AST (D) levels. The relative expression levels of PPARα-related target genes in the livers of LSIRT1$^{-/-}$ mice treated with AM6545 are shown (E). The values represent the percent fold change in expression relative to the WT littermate controls. Data represent the mean ± SEM from 4 to 15 mice per group. *$P < 0.05$ relative to the vehicle-treated group from the same strain. For panels a, original magnification of × 40. Scale bars, 100 μm.

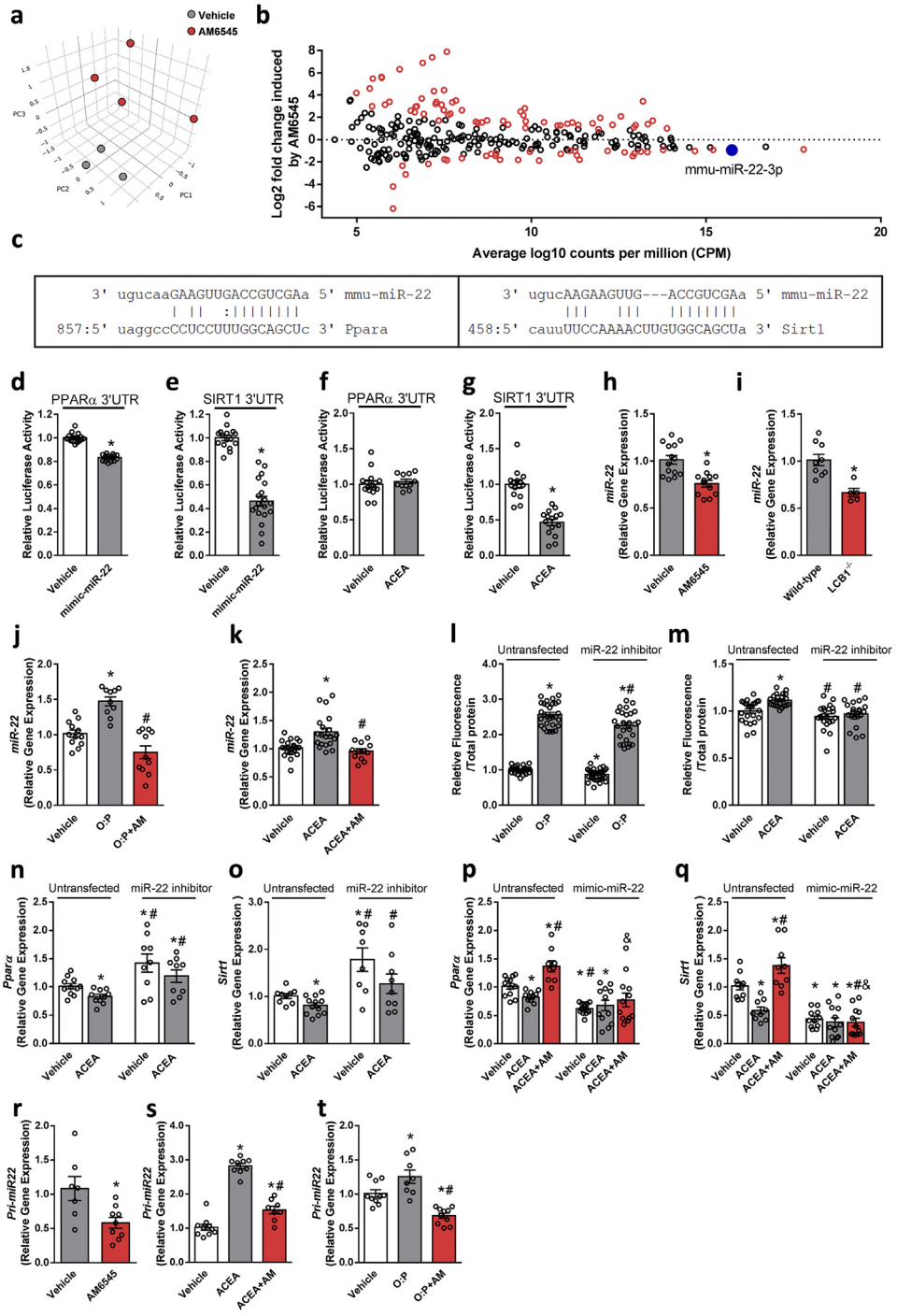

Figure 6: Hepatic CB_1R regulates PPARα and SIRT1 expression via miR-22-3-p. C57Bl/6 mice were fed a HFD for 14 weeks and then treated with AM6545 (10 mg/kg, i.p.) for 1 week. (A—B) miRNA profiles were obtained via deep sequencing of small RNA libraries prepared in house. Principal component analysis based on miR count profiles shows distinct discrimination by treatment (A). The results of miR sequence family differential expression analysis are displayed as an MA plot (B) in which red points denote $P < 0.05$. The mature sequences of miR-22 and base pairing alignments with the 3′ UTR of PPARα (left) and SIRT1 (right) are shown as predicted by miRanda (C). Co-transfection of hepatocytes with mimic-miR-22 and a luciferase reporter containing the 3′UTR sequence of the PPARα and SIRT1 genes that contained miR-22 recognition sequences reduced the luciferase activity of both PPARα (D) and SIRT1 (E). A reduction in luciferase activity in cells containing the 3′UTR sequence of SIRT1 (G) but not PPARα (F) was recorded when the cells were treated with ACEA. One-week treatment with AM6545 (H) or genetic ablation of hepatic CB_1R (I) resulted in significant reductions in hepatic miR-22 levels. Similarly, AM6545 (1 μM) reduced the elevated expression levels of miR-22 in hepatocytes exposed to 0.6 mM oleate and palmitate (O:P = 2:1, respectively, J) or 1 μM ACEA (K) for 24 h. Transient transfection of hepatocytes with a miR-22 hairpin inhibitor reduced the ability of the cells to accumulate fat following exposure to O:P (L) or ACEA (M) treatment. ACEA was unable to reduce the expression of PPARα (N) and SIRT1 (O) in the transfected cells with a miR-22 hairpin inhibitor. AM6545 (1 μM) was unable to prevent the ACEA-induced reduction in PPARα (P) and SIRT1 (Q) in hepatocytes transiently transfected with mimic-miR-22. AM6545 reduced the hepatic expression of pri-mir-22 in DIO mice (R). Similarly, AM6545 (1 μM) reduced the elevated expression levels of pri-mir-22 in hepatocytes exposed to 1 μM ACEA (S) or 0.6 mM oleate and palmitate (O:P, 2:1, respectively, T) for 24 h. *In vitro* data represent the mean ± SEM from 2 to 3 independent experiments. *$P < 0.05$ relative to the vehicle-treated group. #$P < 0.05$ relative to the same treatment in the untransfected group. *In vivo* data represent the mean ± SEM from 5 to 14 mice per group. *$P < 0.05$ relative to the vehicle-treated or wild-type groups.

Testing the metabolic efficacy of peripherally restricted CB_1R blockade in obese LSIRT1$^{-/-}$ mice and their littermates revealed a pattern similar to those found in PPAR$\alpha^{-/-}$ animals. These findings suggest a hepatic SIRT1-independent effect on the ability of AM6545 to reduce body weight and hyperleptinemia and improve glycemic homeostasis (Supplementary Figs. 4a–h). In addition, a SIRT1-dependent effect of peripheral CB_1R blockade to reverse diet-induced hepatic steatosis as manifested by the inability of AM6545 to reduce hepatic triglyceride content and circulating transaminases (Figure 5A–D). Moreover, AM6545 failed to increase the expression of PPARα-related genes in the LSIRT1$^{-/-}$ mice (Figure 5E), further suggesting that a link exists between the CB_1R, SIRT1, and PPARα in modulating fat utilization in the liver.

3.5. Hepatic CB_1R regulates PPARα and SIRT1 via miR22

Emerging evidence suggests that epigenetic alterations, in particular those leading to abnormal microRNA (miR) expression, are implicated in regulating both SIRT1 and PPARs expression or activity in various tissues (reviewed in [43,44]). To decipher whether (and more importantly, which) miRs link CB_1R with SIRT1 and PPARα, we performed miR sequence profiling of liver tissues collected from the DIO mice treated with AM6545 or vehicle (Veh). Principal component analysis (PCA) of these samples by miR profiles, plotted in Figure 6A, suggested that major miR transcriptome alterations exist between the two groups. To identify specific miRs in the liver that are modulated by CB_1R blockade, we evaluated miR differential expression. A total of 269 miRs were confidently detected. While the majority of miRs did not exhibit a significant differential expression between the two groups, several miRs were either over- ($n = 58$) or under-expressed ($n = 32$) in AM6545- compared with Veh-treated animals (Figure 6B). Of those that were significantly dysregulated in the AM6545-treated mice (Supplementary Tables 3 and 4), only miR-22–3p (miR-22), conserved among mammalians (Supplementary Fig. 5) and highly expressed miR in the liver that was significantly downregulated by AM6545, was predicted to target both SIRT1 and PPARα based on six computational methods (DIANA-microT, ElMMo, miRanda, PicTar, Pita, and TargetScan; Figure 6C and Supplementary Tables 3 and 4).

To determine whether miR-22 specifically targets PPARα and SIRT1, we performed *in vitro* functional assays in hepatocytes using a luciferase reporter paired to the 3′UTR sequences of the PPARα and SIRT1 genes, which contain the miR-22 recognition sequence, and tested their repression by activating miR-22 (using mimic-miR-22 overexpression). The overexpression of miR-22 in these cells (Supplementary Fig. 6b) decreased the luciferase activity in hepatocytes transfected with luciferase reporters containing the 3′UTR sequences of PPARα and SIRT1 compared with untransfected cells (Figure 6D,E). Interestingly, when we tested the indirect effect of activating miR-22 via CB_1R agonism, the reduction in luciferase activity following the exposure of hepatocytes to ACEA was only limited to SIRT1 (Figure 6F,G). The reduction in miR-22 expression following either pharmacological blockade or genetic ablation of the CB_1R in the liver was further validated by qPCR *in vivo* (Figure 6H,I) as well as in hepatocytes either exposed to lipotoxic conditions or treated with ACEA (Figure 6J,K). The specific regulatory role of the CB_1R in miR-22 was validated in hepatocytes treated with the highly potent CB_1R and CB_2R agonists HU-210 and HU-308, respectively (Supplementary Fig. 7), demonstrating that this miR is not regulated by the CB_2R. Transfection of hepatocytes with a miR-22 hairpin inhibitor (Supplementary Fig. 6a) led to reduced cellular fat accumulation under lipotoxic and CB_1R agonism conditions (Figure 6L,M). Moreover, hepatocyte transfection with a miR-22 hairpin inhibitor resulted in a diminished ability of ACEA to reduce PPARα and SIRT1 expression (Figure 6N and O). In contrast, AM6545 was unable to reverse the CB_1R-induced downregulation of PPARα and SIRT1 expression in hepatocytes transfected with mimic-miR-22 (Figure 6P and Q and Supplementary Fig. 6b). To determine whether CB_1R regulates miR-22 at the primary transcript level, we assessed the expression of miR-22's primary transcript (pri-miR-22) and found that indeed, chronic and acute blockade of the CB_1R (in DIO mice and hepatocytes, respectively) downregulated its expression in a pattern similar to that of mature miR-22 (Figure 6R–T).

3.6. Hepatic CB_1R regulates miR22 via modulating p53 activity

Since the transcription factor p53 is known to induce changes in miR expression (reviewed in [45]) and its activity was reported to be regulated by the CB_1R [46], we first evaluated p53 expression *in vivo* and found that it was downregulated by either pharmacological blockade or genetic ablation of the CB_1R in hepatocytes (Figure 7A–D). Interestingly, an opposite p53 expression pattern was found when we activated the CB_1R in HepG2 cells using the highly potent CB_1R agonist HU-210 (100 nM); we found that its expression significantly increased in comparison with vehicle-treated cells (Figure 7E,F). We further verified this in immortalized mouse primary hepatocytes treated with ACEA and AM6545 (Figure 7G,H). We next transfected hepatocytes with a GFP reporter gene derived by a p53 transcriptional responsive element paired with a minimal CMV promotor and tested the effect of CB_1R activation/blockade on p53 transcriptional activity. Specific activation of the CB_1R by ACEA increased p53 transcriptional activity in hepatocytes as manifested by the increased GFP fluorescence, an effect that was abolished by pretreating the cells with AM6545 (Figure 7I). We also assessed the mRNA expression of *p21*, *PUMA*, *BAX*, and *miR-34a*, which are known to be directly regulated by p53 [47,48] and found that ACEA increased their expression, whereas AM6545 reduced it (Figure 7J). To actively regulate the transcription of genes, p53 protein must migrate into the nucleus [49]. Therefore, we analyzed the nuclear levels of p53 protein expression following the activation/blockade of the CB_1R in hepatocytes and found elevated levels in CB_1R-activated hepatocytes, an effect that was downregulated by AM6545 treatment (Figure 7K,L). Furthermore, indirect activation of the CB_1R (via inhibiting eCB degradation using JZL195) and by exposing hepatocytes to lipotoxic conditions upregulated the expression of miR-34a, an effect that was completely inhibited by AM6545 (Figure 7M and N). Moreover, CB_1R-induced upregulation of both miR-34a and miR-22 was completely inhibited by pifithrin-α (PFT-α), a reversible transcriptional inhibitor of p53 (Figure 7O and P). To demonstrate the direct regulation of miR-22 by p53, we tested the effect of DOX, a known activator of p53 [50] on miR-22 and found that upregulating the transcriptional activity of p53 by DOX (Figure 7Q) was associated with increased expression of miR-22 (Figure 7R). Taken together, these findings support a molecular link between CB_1R, p53, and miR-22 in hepatocytes.

3.7. Differential hepatic expression profiles of PPARα and SIRT1 in humans with NAFLD

To determine whether our animal findings correlate to humans, we reanalyzed a data set reporting the gene expression profile of PPARα and SIRT1 in liver biopsies obtained from human patients with/without NASH [28,29]. Interestingly, significant reductions in the expression levels of PPARα and SIRT1 were found in patients with NASH compared with controls (Supplementary Figs. 8a and b), further supporting the translational aspects of our findings.

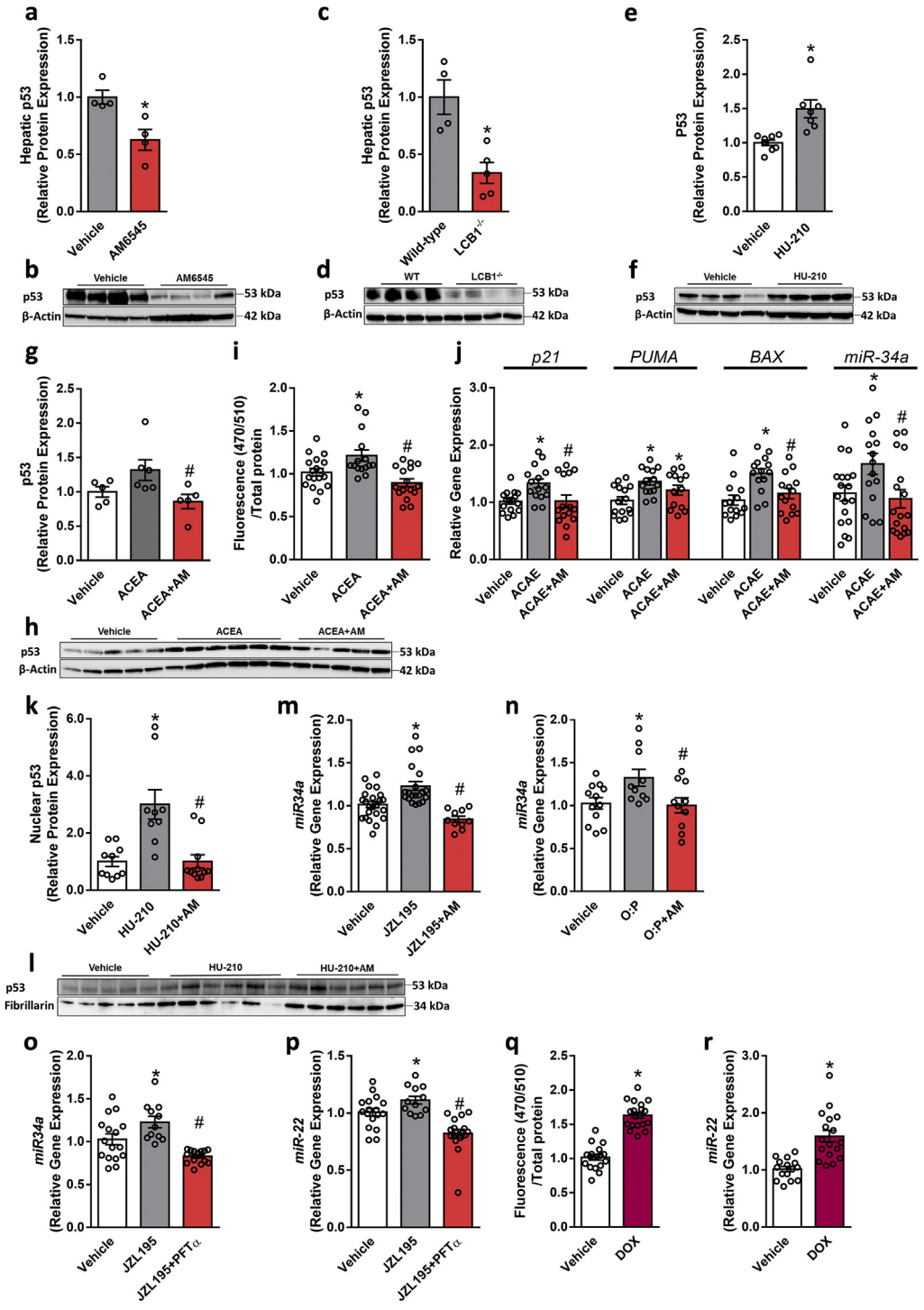

Figure 7: CB_1R regulates miR-22 expression and activity via p53. Male six-week-old C57Bl/6 and $LCB1^{-/-}$ mice were fed a HFD for 14 weeks and then WT obese mice were treated with AM6545 (10 mg/kg, i.p.) for 7 days. Chronic CB_1R blockade (A and B) or genetic ablation of hepatic CB_1R (C and D) in obese mice resulted in reduction in the hepatic protein expression of p53. HU-210 (100 nM) increased the protein expression of p53 in HepG2 cells (E and F), whereas AM6545 (1 μM) prevented the elevated expression levels of p53 induced by ACEA (10 μM) in immortalized mouse primary hepatocytes (G and H). ACEA (10 μM) increased GFP fluorescence in hepatocytes transfected with a lentivector encoding GFP derived by p53 transcriptional response elements paired with a minimal CMV promotor, whereas AM6545 (1 μM) abolished this effect (I). AM6545 (1 μM) also reduced the elevated expression levels of *p21*, *PUMA*, *BAX*, and miR-34a induced by 1 μM ACEA in hepatocytes (J). HU-210 (100 nM) increased the nuclear localization of p53 in hepatocytes, an effect that was prevented by pretreating the cells with AM6545 (1 μM) (K and L). AM6545 (1 μM) prevented the increased expression of miR-34a induced by 250 nM JZL195 (M) or 0.6 mM O:P treatment (N) in hepatocytes. Exposing hepatocytes to PFT-α prevented the JZL195-induced elevation in the expression of miR-34a (O) and miR-22 (P). Doxorubicin (DOX, 1.9 μM) increased GFP fluorescence in hepatocytes transfected with a lentivector encoding GFP derived by p53 transcriptional response elements paired with a minimal CMV promotor (Q). DOX (1.9 μM) also induced elevation in miR-22 expression in hepatocytes (R). *In vitro* data represent the mean ± SEM from 2 to 5 independent experiments. $^{*}P < 0.05$ relative to the vehicle-treated group. $^{\#}P < 0.05$ relative to the ACEA-, O:P-, or JZL195-treated groups. *In vivo* data represent the mean ± SEM from 4 to 9 mice per group. $^{*}P < 0.05$ relative to the vehicle-treated or wild-type groups.

4. DISCUSSION

NAFLD, the most chronic liver disease worldwide, is strongly associated with obesity and insulin resistance; however, to date, the molecular signaling pathways leading to the development of NAFLD are not completely understood. In the current study, we deciphered a new signaling pathway regulated by hepatic CB_1R that contributes to the development of diet-induced hepatic steatosis. It can be targeted by novel peripherally restricted CB_1R antagonists that are currently under preclinical and clinical evaluation. We also provide evidence indicating that hepatic CB_1R increases the regulatory role of p53 on miR-22, which in turn represses the expression and activity of PPARα and SIRT1, further contributing to fat accumulation in hepatocytes.

The hepatic expression of the CB_1R is upregulated in DIO and murine models of fatty liver [3,4,7]. In fact, its presence in hepatocytes is crucial for the development of NAFLD [4]; therefore, centrally acting and peripherally restricted CB_1R antagonists were found to be efficacious in ameliorating hepatic steatosis in both humans [9,51] and animals [6,8,52]. To elucidate the underlying molecular mechanism by which the CB_1R contributes to NAFLD, we used an unbiased approach utilizing NPP analysis to identify multiple genes that display a conservation pattern across phylogenetic clades similar to those of the CB_1R. In doing so, we hypothesized that genes that are coevolved with the CB_1R are functionally linked [13]. Indeed, most of the genes found are related to proteins associated with regulating energy homeostasis, fertility, and longevity. These findings are in line with the fact that the eCB system evolved to conserve energy in situations of food deprivation [53] and the documented role of this system in regulating energy homeostasis by promoting caloric intake, energy storage, and fat accumulation via activating the CB_1R in the central nervous system as well as in peripheral tissues.

Among the genes that coevolved with the CB_1R, we identified PPARα, a master regulator of lipid metabolism that is abundantly expressed in the liver, as the highest scored gene associated with NAFLD. Not only did we provide evidence that stimulating hepatic CB_1R reduces the expression and activity of PPARα in cultured hepatocytes, we also demonstrated that pharmacological blockade or genetic ablation of hepatic CB_1R upregulates PPARα expression and activity in DIO mice. Although the connection between PPARs and eCBs is well established (reviewed in [54]), very few studies have investigated the specific effect of the CB_1R on PPARα. Similar to our work, studies that reported the efficacy of the globally acting CB_1R inverse agonists rimonabant and AM251 in DIO mice found an increased expression of hepatic PPARα and its downstream target genes [10,55]. Reports regarding the role of the CB_1R in regulating PPARα in visceral adipose tissue are conflicting, since rimonabant increases the expression of PPARα in DIO mice [55], whereas LH-1, a CB_1R antagonist with a low affinity to the CB_1R, reduces adipocyte PPARα expression [56]. Although LH-1 has the ability to reduce body weight, it failed to ameliorate hepatic steatosis and hypertriglyceridemia in obese Zucker rats [57]. In comparison with LH-1, our tested compound AM6545 reversed diet-induced hepatic steatosis and liver injury via PPARα since it completely failed to induce all of these effects in PPARα null mice. These results are in line with several studies indicating that PPARα activation is hepatoprotective. For instance, several PPARα agonists, such as Wy-14, 643, and fenofibrate, were found to prevent the development of hepatic steatosis in animal models of NAFLD [58,59]. Conversely, PPARα deletion predisposes mice to develop fatty liver under a regular diet and HFD conditions [34,35,60,61].

As previously mentioned, accumulating evidence indicates that most cannabinoid (both endo and phyto) molecules interact with PPARs by directly binding to these nuclear receptors, by the catabolism of cannabinoids to PPAR-activating chemicals or by indirectly activating PPARs via distinct molecular signaling pathways (reviewed in [62]). It was even suggested that non-Δ^9-tetrahydrocannbidiol (THC) phytocannabinoids, such as cannabigerolic acid (CBGA), cannabidiolic acid (CBDA), and cannabigerol (CBG), directly activate PPARα, modulate its target genes associated with lipid metabolism, and reduce lipid accumulation in hepatocytes [63]. Herein, we report that AM6545 neither binds nor activates (directly or allosterically) PPARα, suggesting that its effect in modulating PPARα expression and activity is mediated via blocking the CB_1R in hepatocytes. Nevertheless, our findings also support an indirect effect of the CB_1R on PPARα via modulating the hepatic levels of AEA and the eCB-like molecules, OEA and PEA, both of which are known as PPARα agonists [54]. Whereas their blood, brain, adipose, and duodenal levels have been shown to increase in obese animals and humans [64,65], we show that their hepatic levels in DIO mice are elevated following either pharmacological blockade or genetic deletion of the CB_1R in hepatocytes. These findings may suggest a link between the CB_1R and their biosynthesis and/or degradation. However, AM6545 was not found to affect FAAH or MAGL activity; thus, further studies will need to identify the molecular mechanism by which the CB_1R regulates the levels of AEA, OEA, and PEA in the liver. In the context of the current work, the hepatic upregulation in the AEA levels is less important, since its expected lipogenic activity is most likely negated in the presence of AM6545 or in mice lacking the CB_1R in hepatocytes. However, amelioration of hepatic steatosis by blocking the CB_1R can be mediated via upregulating the levels of OEA and PEA, whose antisteatotic effect was previously reported [38,66–68]. Specifically, both are known to regulate the expression of PPARα target genes implicated in FFA mobilization and oxidation and affect mitochondrial flexibility in hepatocytes [66,69]. In fact, OEA has been shown to stimulate FFA β-oxidation and reduce the triglyceride content in adipose tissue and the liver [69], and its anorectic and lipolytic properties have been synergistically enhanced by the CB_1R antagonist rimonabant [70]. Therefore, antagonizing the CB_1R should be a more efficacious strategy than using phytocannabinoids, eCB-like molecules *per se*, or inhibitors of AEA biosynthesis [71,72], which also inhibit the action of OEA and PEA at hepatic PPARα, further supporting the use of peripheral CB_1R blockers to treat obesity-induced fatty liver disease.

In this study, we also found that either direct or indirect activation of the CB_1R reduces the expression and activity of hepatic SIRT1, which may also contribute to fat accumulation within hepatocytes. Our observation that AM6545 prevents the fatty acid-induced reduction in SIRT1 expression indicates that this effect is mediated by the CB_1R. Moreover, CB_1R blockade or its genetic ablation from hepatocytes increased the expression and activity of SIRT1, further indicating a negative relationship between these two proteins. The existing evidence suggesting a link between CB_1R and SIRT1 remains controversial. In human primary chondrocytes, ACEA prevented a reduction in SIRT1 expression induced by interleukin-1β; however, the sole effect of ACEA on SIRT1 expression was not reported in this study [73]. In line with our findings, ACEA was found to reduce the expression of SIRT1 in primary mouse hepatocytes and the HepG2 cell line [74]. Others have found that fatty acid flux reduces the expression of SIRT1 and induces fat accumulation in normal human hepatocytes [75]. Moreover, our findings indicate that the improvement in hepatic steatosis by peripheral CB_1R blockade is accompanied by increased expression and activity of hepatic SIRT1. In fact, it depends specifically on its presence in hepatocytes, further providing evidence that the CB_1R negatively regulates SIRT1.However, Liu et al. recently reported that JD5037, a

peripherally restricted CB_1R inverse agonist, improves hepatic steatosis in mice lacking SIRT1, specifically in hepatocytes [74]. The difference in the results between this study and ours could be explained by the physiochemical properties of the two compounds (a neutral antagonist vs an inverse agonist). Nevertheless, multiple studies pinpoint the protective role of SIRT1 against the development of fatty liver. For instance, heterozygous SIRT1 knockout mice accumulate more fat in their livers than their wild-type littermates [76]; specific deletion of exons 5 and 6 of the *Sirt1* gene in the liver predisposes mice to develop fatty liver with a regular diet [77]. Impaired hepatic PPARα signaling and a tendency toward fat accumulation in the liver were reported in mice carrying a deletion of exon 4 of *Sirt1* gene in mice [22]. In fact, SIRT1 is known to interact with PPARα, and its overexpression increases the transcriptional activity of PPARα in hepatocytes [22]. These findings are consistent with our results, which showed that AM6545 increased the expression of PPARα target genes in the livers of the wild-type mice but failed to do so in the $LSIRT1^{-/-}$ mice. It is worth mentioning that in our study, both the obese PPARα and LSIRT1 null mice did not exhibit increased susceptibility to hepatic steatosis compared with their WT littermate controls. Trends toward an elevation in ALT and AST levels were found, but they did not reach significance. These results could be explained by the different composition of fatty acids in the HFD used to induce obesity and fatty liver in these animals. However, the inability of AM6545 to ameliorate hepatic steatosis in the null mice supports our general hypothesis. We also report the presence of a similar expression profile of PPARα and SIRT1 (downregulation) in liver samples collected from patients with NASH. Regarding PPARα, its decreased hepatic expression levels in humans with NAFLD were previously reported and were found to increase in parallel with NAFLD histological improvement secondary to lifestyle intervention or bariatric surgery [78]. Similarly, direct evidence of the downregulation of SIRT1 in the liver of NAFLD patients was correlated with increased expression of hepatic *de novo* lipogenesis [79]. Although not reported here, others have shown an increased expression of the CB_1R in patients with NAFLD/NASH [80]; this evidence supports the rationale of blocking this receptor for therapeutic benefits in these clinical conditions.

Aberrant miR expression is associated with NAFLD, and emerging evidence suggests that miRs play a crucial role in the development of NAFLD [81]. Herein, we observed that improvement in hepatic steatosis induced by AM6545 was accompanied by alterations in the expression of several hepatic miRs, which may further imply a role for miRs in the pathogenesis of NAFLD and its reversal. We specifically found that miR-22 is regulated by the CB_1R since it was downregulated by either pharmacological blockade or genetic deletion of hepatic CB_1R. Furthermore, activation of the CB_1R or fatty acid flux increases its expression in a CB_1R-dependent manner, which in turn directly regulates PPARα and SIRT1 and contributes to fat accumulation in hepatocytes. Previous data indicated elevated circulating and hepatic miR-22 levels in humans with fatty liver compared with normal livers [82,83] and suggest a key role of miR-22 in the induction of hepatic steatosis [83]. Our novel findings regarding the regulation of hepatic PPARα and SIRT1 by miR-22 are supported by other studies that also found a similar interaction between these molecules in other organs/cells. PPARα and SIRT1 expression levels were found to be reduced in mice overexpressing miR-22 in cardiomyocytes and elevated in the hearts of miR-22 null mice [84]. Similarly, miR-22 was found to regulate PPARα and SIRT1 mRNA expression levels in mouse embryonic fibroblasts [84], chondrocytes [85], glioblastoma cell lines [86], and breast cancer cell lines [87]. Furthermore, butyrate was found to increase miR-22 expression, which in turn reduced SIRT1 in the human hepatocellular carcinoma cell line Huh7 cells [88].

At the molecular signaling level, we also found that CB_1R activation increased the transcription of pri-miR-22 in hepatocytes, whereas its blockade reduced the hepatic pri-miR-22 expression in the DIO mice, indicating that the CB_1R affects miR-22 at the transcriptional level. This is most likely achieved via inducing changes in the expression, acetylation, localization, and activity of p53, a transcription factor that upregulates the expression of miR-22 [89]. In fact, a positive correlation of p53 expression and the severity of NAFLD was previously reported in humans [90], and its induction as measured by increased nuclear localization and enhanced p21 expression was reported in two mouse models of fatty liver disease [91]. However, the role of p53 in the development of hepatic steatosis remains controversial, since studies indicating the prosteatotic effect of p53 exist (as previously mentioned), along with reports suggesting a hepatoprotective role of p53 (reviewed in [92,93]).

Interestingly, all of the findings presented herein suggest the direct positive regulation of p53 by the CB_1R in the liver. First, we described changes in the transcriptional expression of p53 in hepatocytes/liver following stimulation, pharmacological blockade, or genetic deletion of the CB_1R. Upregulation of p53 expression by stimulating the CB_1R further translated to enhanced transcriptional activity as manifested by the increased localization of p53 in the cell nucleus and the amplified expression of its target genes *miR-34a*, *p21*, *PUMA*, and *BAX*, known to induce cellular arrest, death, and senescence [94]. In fact, excess levels of p53 have been suggested to lead to the aforementioned undesired cellular fates, including hepatocyte injury and cell death, both of which were strongly linked to NAFLD progression [93].

Second, our findings indicate that the direct activation of p53 (by DOX) upregulates miR-22 expression. Such elevation was also achieved by stimulating the CB_1R, an effect that failed to increase the expression of miR-22 and miR-34a in the presence of PTF-α, a p53 transcriptional activity inhibitor. These observations are in line with reports that THC, a CB_1R partial agonist, induces the activation of p53 in neurons [46]. In support of our findings, Derdak et al. found that pharmacological treatment with PFT-α reduced DIO-induced hepatic steatosis by reducing miR-34a, which was followed by increased expression of SIRT1 and enhanced PPARα transcriptional activation [95]. Moreover, miR-34a contributes to the development of hepatic steatosis by directly inhibiting SIRT1 and PPARα expression in mouse models of diet-induced hepatic steatosis and HepG2 cells [75]. Since the role of miR-34a in promoting hepatic steatosis has already been identified [96], our current finding that CB_1R stimulation promotes miR-34a expression via p53 activation may imply the existence of another plausible mechanism by which hepatic CB_1R regulates PPARα and SIRT1 and contributes to fat accumulation in the liver. However, further research is needed to establish this link.

Finally, of significant relevance to p53 activity, activation of the CB_1R also elevated acetylated levels of p53. However, in the context of the current findings, this observation was associated with a CB_1R-mediated reduction in SIRT1 activity. Yet, p53 acetylation was previously reported to increase its stability, its binding to low-affinity promoters, its association with multiple proteins, and more [94]. Specifically, acetylation of p53 directly affects its transcriptional activity by opening its usually closed configuration or altering its binding to several response elements in gene targets [94]. Therefore, it could be postulated that its increased acetylation in hepatocytes treated with the CB_1R agonist ACEA or when exposed to lipotoxic conditions may also augment the association of p53 with the Drosha microRNA processor and promote nuclear primary miR-22 expression, maturation, and

stability, as was reported for other miRs [97]. However, miR-22 may directly regulate the activity and function as well as contribute to the fine-tuning of p53 as reported for miR-34a, miR-122, miR-24, and miR-1228 (reviewed in [93]). However, substantially more research is needed to elucidate the physiological interaction of miR-22 and p53 and its implication in the development of NAFLD.

5. CONCLUSIONS

In conclusion, ameliorating DIO-induced hepatic steatosis by peripherally restricted CB_1R blockade was found to be PPARα and SIRT1 dependent. Furthermore, modulating their hepatic expression and activity by the CB_1R was directly controlled via a p53/miR-22 signaling pathway, resulting in changes in lipid utilization within hepatocytes. In parallel, antagonizing the CB_1R may increase hepatic OEA and PEA, which may then directly activate PPARα, resulting in enhanced efficacy in ameliorating hepatic steatosis (Graphical Abstract). Taken together, our findings suggest the existence of a novel molecular signaling pathway by which the CB_1R regulates hepatic lipid homeostasis.

AUTHOR CONTRIBUTIONS

S.A. and J.T. designed, conducted, and supervised the experiments and analyzed the data. S.U., A.D., R.H., and A.N. assisted in conducting the experiments. K.V.V., X.L., and A.M. provided reagents and animals. Y.A. and D.B.Z. performed the human analysis. M.M., D.S.R., and Y.T. conducted the NPP analysis. D.G.W. and I.Z.B.D.performed the miR transcript analysis. S.A., Y.T., I.Z.B.D., and J.T. wrote the manuscript.

ACKNOWLEDGMENTS

This study was supported by an Israel Science Foundation (ISF) grant (#158/18) to J.T.

CONFLICT OF INTEREST

The authors declare no conflicts of interest.

APPENDIX A. SUPPLEMENTARY DATA

Supplementary data to this article can be found online at https://doi.org/10.1016/j.molmet.2020.101087.

REFERENCES

[1] Adinolfi, L.E., Marrone, A., Rinaldi, L., 2018. Non-alcoholic fatty liver disease: beyond the liver is an emerging multifaceted systemic disease. Hepatobiliary Surgery and Nutrition 7:143–146.

[2] Tam, J., Liu, J., Mukhopadhyay, B., Cinar, R., Godlewski, G., Kunos, G., 2011. Endocannabinoids in liver disease. Hepatology 53:346–355.

[3] Osei-Hyiaman, D., DePetrillo, M., Pacher, P., Liu, J., Radaeva, S., Batkai, S., et al., 2005. Endocannabinoid activation at hepatic CB1 receptors stimulates fatty acid synthesis and contributes to diet-induced obesity. Journal of Clinical Investigation 115:1298–1305.

[4] Osei-Hyiaman, D., Liu, J., Zhou, L., Godlewski, G., Harvey-White, J., Jeong, W.I., et al., 2008. Hepatic CB1 receptor is required for development of diet-induced steatosis, dyslipidemia, and insulin and leptin resistance in mice. Journal of Clinical Investigation 118:3160–3169.

[5] Liu, J., Zhou, L., Xiong, K., Godlewski, G., Mukhopadhyay, B., Tam, J., et al., 2012. Hepatic cannabinoid receptor-1 mediates diet-induced insulin resistance via inhibition of insulin signaling and clearance in mice. Gastroenterology 142:1218–1228 e1.

[6] Tam, J., Vemuri, V.K., Liu, J., Batkai, S., Mukhopadhyay, B., Godlewski, G., et al., 2010. Peripheral CB1 cannabinoid receptor blockade improves cardiometabolic risk in mouse models of obesity. Journal of Clinical Investigation 120:2953–2966.

[7] Jourdan, T., Djaouti, L., Demizieux, L., Gresti, J., Verges, B., Degrace, P., 2010. CB1 antagonism exerts specific molecular effects on visceral and subcutaneous fat and reverses liver steatosis in diet-induced obese mice. Diabetes 59:926–934.

[8] Tam, J., Godlewski, G., Earley, B.J., Zhou, L., Jourdan, T., Szanda, G., et al., 2014. Role of adiponectin in the metabolic effects of cannabinoid type 1 receptor blockade in mice with diet-induced obesity. American Journal of Physiology. Endocrinology and Metabolism 306:E457–E468.

[9] Despres, J.P., Ross, R., Boka, G., Almeras, N., Lemieux, I., Investigators, A.D.-L., 2009. Effect of rimonabant on the high-triglyceride/low-HDL-cholesterol dyslipidemia, intraabdominal adiposity, and liver fat: the ADAGIO-Lipids trial. Arteriosclerosis, Thrombosis, and Vascular Biology 29:416–423.

[10] Zhao, W., Fong, O., Muise, E.S., Thompson, J.R., Weingarth, D., Qian, S., et al., 2010. Genome-wide expression profiling revealed peripheral effects of cannabinoid receptor 1 inverse agonists in improving insulin sensitivity and metabolic parameters. Molecular Pharmacology 78:350–359.

[11] Tabach, Y., Billi, A.C., Hayes, G.D., Newman, M.A., Zuk, O., Gabel, H., et al., 2013. Identification of small RNA pathway genes using patterns of phylogenetic conservation and divergence. Nature 493:694–698.

[12] Tabach, Y., Golan, T., Hernandez-Hernandez, A., Messer, A.R., Fukuda, T., Kouznetsova, A., et al., 2013. Human disease locus discovery and mapping to molecular pathways through phylogenetic profiling. Molecular Systems Biology 9:692.

[13] Sadreyev, I.R., Ji, F., Cohen, E., Ruvkun, G., Tabach, Y., 2015. PhyloGene server for identification and visualization of co-evolving proteins using normalized phylogenetic profiles. Nucleic Acids Research 43:W154–W159.

[14] Sherill-Rofe, D., Rahat, D., Findlay, S., Mellul, A., Guberman, I., Braun, M., et al., 2019. Mapping global and local coevolution across 600 species to identify novel homologous recombination repair genes. Genome Research 29:439–448.

[15] UniProt, C., 2019. UniProt: a worldwide hub of protein knowledge. Nucleic Acids Research 47:D506–D515.

[16] O'Leary, N.A., Wright, M.W., Brister, J.R., Ciufo, S., Haddad, D., McVeigh, R., et al., 2016. Reference sequence (RefSeq) database at NCBI: current status, taxonomic expansion, and functional annotation. Nucleic Acids Research 44:D733–D745.

[17] Camacho, C., Coulouris, G., Avagyan, V., Ma, N., Papadopoulos, J., Bealer, K., et al., 2009. BLAST+: architecture and applications. BMC Bioinformatics 10:421.

[18] Altschul, S.F., Gish, W., Miller, W., Myers, E.W., Lipman, D.J., 1990. Basic local alignment search tool. Journal of Molecular Biology 215:403–410.

[19] Enault, F., Suhre, K., Poirot, O., Abergel, C., Claverie, J.M., 2004. Phydbac2: improved inference of gene function using interactive phylogenomic profiling and chromosomal location analysis. Nucleic Acids Research 32:W336–W339.

[20] Kilkenny, C., Browne, W., Cuthill, I.C., Emerson, M., Altman, D.G., Group, N.C.R.R.G.W., 2010. Animal research: reporting in vivo experiments: the ARRIVE guidelines. British Journal of Pharmacology 160:1577–1579.

[21] Akiyama, T.E., Nicol, C.J., Fievet, C., Staels, B., Ward, J.M., Auwerx, J., et al., 2001. Peroxisome proliferator-activated receptor-alpha regulates lipid homeostasis, but is not associated with obesity: studies with congenic mouse lines. Journal of Biological Chemistry 276:39088–39093.

[22] Purushotham, A., Schug, T.T., Xu, Q., Surapureddi, S., Guo, X., Li, X., 2009. Hepatocyte-specific deletion of SIRT1 alters fatty acid metabolism and results in hepatic steatosis and inflammation. Cell Metabolism 9:327—338.
[23] Folch, J., Lees, M., Sloane Stanley, G.H., 1957. A simple method for the isolation and purification of total lipides from animal tissues. Journal of Biological Chemistry 226:497—509.
[24] Uzi, D., Barda, L., Scaiewicz, V., Mills, M., Mueller, T., Gonzalez-Rodriguez, A., et al., 2013. CHOP is a critical regulator of acetaminophen-induced hepatotoxicity. Journal of Hepatology 59:495—503.
[25] Mazeh, H., Deutch, T., Karas, A., Bogardus, K.A., Mizrahi, I., Gur-Wahnon, D., et al., 2018. Next-Generation sequencing identifies a highly accurate miRNA panel that distinguishes well-differentiated thyroid cancer from benign thyroid nodules. Cancer Epidemiology Biomarkers & Prevention 27:858—863.
[26] Farazi, T.A., Brown, M., Morozov, P., Ten Hoeve, J.J., Ben-Dov, I.Z., Hovestadt, V., et al., 2012. Bioinformatic analysis of barcoded cDNA libraries for small RNA profiling by next-generation sequencing. Methods 58:171—187.
[27] Azar, S., Sherf-Dagan, S., Nemirovski, A., Webb, M., Raziel, A., Keidar, A., et al., 2019. Circulating endocannabinoids are reduced following bariatric surgery and associated with improved metabolic homeostasis in humans. Obesity Surgery 29:268—276.
[28] Ahrens, M., Ammerpohl, O., von Schonfels, W., Kolarova, J., Bens, S., Itzel, T., et al., 2013. DNA methylation analysis in nonalcoholic fatty liver disease suggests distinct disease-specific and remodeling signatures after bariatric surgery. Cell Metabolism 18:296—302.
[29] Haas, J.T., Vonghia, L., Mogilenko, D.A., Verrijken, A., Molendi-Coste, O., Fleury, S., et al., 2019. Transcriptional network analysis implicates altered hepatic immune function in NASH development and resolution. Nat Metab 1: 604—614.
[30] Anders, S., Huber, W., 2010. Differential expression analysis for sequence count data. Genome Biology 11:R106.
[31] McCarthy, D.J., Chen, Y., Smyth, G.K., 2012. Differential expression analysis of multifactor RNA-Seq experiments with respect to biological variation. Nucleic Acids Research 40:4288—4297.
[32] Ben-Ari Fuchs, S., Lieder, I., Stelzer, G., Mazor, Y., Buzhor, E., Kaplan, S., et al., 2016. GeneAnalytics: an integrative gene set analysis tool for next generation sequencing, RNAseq and microarray data. OMICS 20:139—151.
[33] Pawlak, M., Lefebvre, P., Staels, B., 2015. Molecular mechanism of PPARalpha action and its impact on lipid metabolism, inflammation and fibrosis in non-alcoholic fatty liver disease. Journal of Hepatology 62:720—733.
[34] Abdelmegeed, M.A., Yoo, S.H., Henderson, L.E., Gonzalez, F.J., Woodcroft, K.J., Song, B.J., 2011. PPARalpha expression protects male mice from high fat-induced nonalcoholic fatty liver. Journal of Nutrition 141:603—610.
[35] Stienstra, R., Mandard, S., Patsouris, D., Maass, C., Kersten, S., Muller, M., 2007. Peroxisome proliferator-activated receptor alpha protects against obesity-induced hepatic inflammation. Endocrinology 148:2753—2763.
[36] Kozak, K.R., Gupta, R.A., Moody, J.S., Ji, C., Boeglin, W.E., DuBois, R.N., et al., 2002. 15-Lipoxygenase metabolism of 2-arachidonylglycerol. Generation of a peroxisome proliferator-activated receptor alpha agonist. Journal of Biological Chemistry 277:23278—23286.
[37] Fu, J., Gaetani, S., Oveisi, F., Lo Verme, J., Serrano, A., Rodriguez De Fonseca, F., et al., 2003. Oleylethanolamide regulates feeding and body weight through activation of the nuclear receptor PPAR-alpha. Nature 425:90—93.
[38] Fu, J., Oveisi, F., Gaetani, S., Lin, E., Piomelli, D., 2005. Oleoylethanolamide, an endogenous PPAR-alpha agonist, lowers body weight and hyperlipidemia in obese rats. Neuropharmacology 48:1147—1153.
[39] Lo Verme, J., Fu, J., Astarita, G., La Rana, G., Russo, R., Calignano, A., et al., 2005. The nuclear receptor peroxisome proliferator-activated receptor-alpha mediates the anti-inflammatory actions of palmitoylethanolamide. Molecular Pharmacology 67:15—19.
[40] LoVerme, J., Russo, R., La Rana, G., Fu, J., Farthing, J., Mattace-Raso, G., et al., 2006. Rapid broad-spectrum analgesia through activation of peroxisome proliferator-activated receptor-alpha. Journal of Pharmacology and Experimental Therapeutics 319:1051—1061.
[41] Sun, Y., Alexander, S.P., Kendall, D.A., Bennett, A.J., 2006. Cannabinoids and PPARalpha signalling. Biochemical Society Transactions 34:1095—1097.
[42] Feige, J.N., Lagouge, M., Canto, C., Strehle, A., Houten, S.M., Milne, J.C., et al., 2008. Specific SIRT1 activation mimics low energy levels and protects against diet-induced metabolic disorders by enhancing fat oxidation. Cell Metabolism 8:347—358.
[43] Choi, S.E., Kemper, J.K., 2013. Regulation of SIRT1 by microRNAs. Molecular Cell 36:385—392.
[44] Portius, D., Sobolewski, C., Foti, M., 2017. MicroRNAs-dependent regulation of PPARs in metabolic diseases and cancers. PPAR Research 2017:7058424.
[45] Liu, J., Zhang, C., Zhao, Y., Feng, Z., 2017. MicroRNA control of p53. Journal of Cellular Biochemistry 118:7—14.
[46] Downer, E.J., Gowran, A., Murphy, A.C., Campbell, V.A., 2007. The tumour suppressor protein, p53, is involved in the activation of the apoptotic cascade by Delta9-tetrahydrocannabinol in cultured cortical neurons. European Journal of Pharmacology 564:57—65.
[47] Chang, T.C., Wentzel, E.A., Kent, O.A., Ramachandran, K., Mullendore, M., Lee, K.H., et al., 2007. Transactivation of miR-34a by p53 broadly influences gene expression and promotes apoptosis. Molecular Cell 26:745—752.
[48] McCubrey, J.A., Lertpiriyapong, K., Fitzgerald, T.L., Martelli, A.M., Cocco, L., Rakus, D., et al., 2017. Roles of TP53 in determining therapeutic sensitivity, growth, cellular senescence, invasion and metastasis. Adv Biol Regul 63:32—48.
[49] Shaulsky, G., Goldfinger, N., Ben-Ze'ev, A., Rotter, V., 1990. Nuclear accumulation of p53 protein is mediated by several nuclear localization signals and plays a role in tumorigenesis. Molecular and Cellular Biology 10:6565—6577.
[50] McSweeney, K.M., Bozza, W.P., Alterovitz, W.L., Zhang, B., 2019. Transcriptomic profiling reveals p53 as a key regulator of doxorubicin-induced cardiotoxicity. Cell Death & Disease 5:102.
[51] Wierzbicki, A.S., Pendleton, S., McMahon, Z., Dar, A., Oben, J., Crook, M.A., et al., 2011. Rimonabant improves cholesterol, insulin resistance and markers of non-alcoholic fatty liver in morbidly obese patients: a retrospective cohort study. International Journal of Clinical Practice 65:713—715.
[52] Gary-Bobo, M., Elachouri, G., Gallas, J.F., Janiak, P., Marini, P., Ravinet-Trillou, C., et al., 2007. Rimonabant reduces obesity-associated hepatic steatosis and features of metabolic syndrome in obese Zucker fa/fa rats. Hepatology 46:122—129.
[53] Ruiz de Azua, I., Lutz, B., 2019. Multiple endocannabinoid-mediated mechanisms in the regulation of energy homeostasis in brain and peripheral tissues. Cellular and Molecular Life Sciences 76:1341—1363.
[54] O'Sullivan, S.E., 2016. An update on PPAR activation by cannabinoids. British Journal of Pharmacology 173:1899—1910.
[55] Wei, L.W., Yuan, Z.Q., Zhao, M.D., Gu, C.W., Han, J.H., Fu, L., 2018. Inhibition of cannabinoid receptor 1 can influence the lipid metabolism in mice with diet-induced obesity. Biochemistry 83:1279—1287.
[56] Alonso, M., Serrano, A., Vida, M., Crespillo, A., Hernandez-Folgado, L., Jagerovic, N., et al., 2012. Anti-obesity efficacy of LH-21, a cannabinoid CB(1) receptor antagonist with poor brain penetration, in diet-induced obese rats. British Journal of Pharmacology 165:2274—2291.
[57] Pavon, F.J., Serrano, A., Perez-Valero, V., Jagerovic, N., Hernandez-Folgado, L., Bermudez-Silva, F.J., et al., 2008. Central versus peripheral antagonism of cannabinoid CB1 receptor in obesity: effects of LH-21, a peripherally acting neutral cannabinoid receptor antagonist, in Zucker rats. Journal of Neuroendocrinology 20(Suppl 1):116—123.
[58] Ip, E., Farrell, G.C., Robertson, G., Hall, P., Kirsch, R., Leclercq, I., 2003. Central role of PPARalpha-dependent hepatic lipid turnover in dietary steatohepatitis in mice. Hepatology 38:123—132.
[59] Zhang, N., Lu, Y., Shen, X., Bao, Y., Cheng, J., Chen, L., et al., 2015. Fenofibrate treatment attenuated chronic endoplasmic reticulum stress in the liver of nonalcoholic fatty liver disease mice. Pharmacology 95:173—180.

[60] Costet, P., Legendre, C., More, J., Edgar, A., Galtier, P., Pineau, T., 1998. Peroxisome proliferator-activated receptor alpha-isoform deficiency leads to progressive dyslipidemia with sexually dimorphic obesity and steatosis. Journal of Biological Chemistry 273:29577—29585.

[61] Patsouris, D., Reddy, J.K., Muller, M., Kersten, S., 2006. Peroxisome proliferator-activated receptor alpha mediates the effects of high-fat diet on hepatic gene expression. Endocrinology 147:1508—1516.

[62] Pistis, M., O'Sullivan, S.E., 2017. The role of nuclear hormone receptors in cannabinoid function. Advances in Pharmacology 80:291—328.

[63] D'Aniello, E., Fellous, T., Iannotti, F.A., Gentile, A., Allara, M., Balestrieri, F., et al., 2019. Identification and characterization of phytocannabinoids as novel dual PPARalpha/gamma agonists by a computational and in vitro experimental approach. Biochimica et Biophysica Acta (BBA) - General Subjects 1863:586—597.

[64] Izzo, A.A., Piscitelli, F., Capasso, R., Marini, P., Cristino, L., Petrosino, S., et al., 2010. Basal and fasting/refeeding-regulated tissue levels of endogenous PPAR-alpha ligands in Zucker rats. Obesity 18:55—62.

[65] Annuzzi, G., Piscitelli, F., Di Marino, L., Patti, L., Giacco, R., Costabile, G., et al., 2010. Differential alterations of the concentrations of endocannabinoids and related lipids in the subcutaneous adipose tissue of obese diabetic patients. Lipids in Health and Disease 9:43.

[66] Annunziata, C., Lama, A., Pirozzi, C., Cavaliere, G., Trinchese, G., Di Guida, F., et al., 2020. Palmitoylethanolamide counteracts hepatic metabolic inflexibility modulating mitochondrial function and efficiency in diet-induced obese mice. The FASEB Journal 34:350—364.

[67] Tutunchi, H., Ostadrahimi, A., Saghafi-Asl, M., Hosseinzadeh-Attar, M.J., Shakeri, A., Asghari-Jafarabadi, M., et al., 2020. Oleoylethanolamide supplementation in obese patients newly diagnosed with non-alcoholic fatty liver disease: effects on metabolic parameters, anthropometric indices, and expression of PPAR-alpha, UCP1, and UCP2 genes. Pharmacological Research 156:104770.

[68] Li, L., Li, L., Chen, L., Lin, X., Xu, Y., Ren, J., et al., 2015. Effect of oleoylethanolamide on diet-induced nonalcoholic fatty liver in rats. Journal of Pharmacological Sciences 127:244—250.

[69] Guzman, M., Lo Verme, J., Fu, J., Oveisi, F., Blazquez, C., Piomelli, D., 2004. Oleoylethanolamide stimulates lipolysis by activating the nuclear receptor peroxisome proliferator-activated receptor alpha (PPAR-alpha). Journal of Biological Chemistry 279:27849—27854.

[70] Serrano, A., Del Arco, I., Javier Pavon, F., Macias, M., Perez-Valero, V., Rodriguez de Fonseca, F., 2008. The cannabinoid CB1 receptor antagonist SR141716A (Rimonabant) enhances the metabolic benefits of long-term treatment with oleoylethanolamide in Zucker rats. Neuropharmacology 54:226—234.

[71] Castellani, B., Diamanti, E., Pizzirani, D., Tardia, P., Maccesi, M., Realini, N., et al., 2017. Synthesis and characterization of the first inhibitor of N-acyl-phosphatidylethanolamine phospholipase D (NAPE-PLD). Chemical Communications 53:12814—12817.

[72] Mock, E.D., Mustafa, M., Gunduz-Cinar, O., Cinar, R., Petrie, G.N., Kantae, V., et al., 2020. Discovery of a NAPE-PLD inhibitor that modulates emotional behavior in mice. Nature Chemical Biology 16:667—675.

[73] Zhang, D., Zhang, G., Li, Z., Li, B., 2018. Activation of the cannabinoid receptor 1 by ACEA suppresses senescence in human primary chondrocytes through sirt1 activation. Experimental Biology and Medicine 243:437—443.

[74] Liu, J., Godlewski, G., Jourdan, T., Liu, Z., Cinar, R., Xiong, K., et al., 2019. Cannabinoid-1 receptor antagonism improves glycemic control and increases energy expenditure through sirtuin-1/mechanistic target of rapamycin complex 2 and 5'Adenosine monophosphate-activated protein kinase signaling. Hepatology 69:1535—1548.

[75] Ding, J., Li, M., Wan, X., Jin, X., Chen, S., Yu, C., et al., 2015. Effect of miR-34a in regulating steatosis by targeting PPARalpha expression in nonalcoholic fatty liver disease. Scientific Reports 5:13729.

[76] Xu, F., Gao, Z., Zhang, J., Rivera, C.A., Yin, J., Weng, J., et al., 2010. Lack of SIRT1 (Mammalian Sirtuin 1) activity leads to liver steatosis in the SIRT1+/- mice: a role of lipid mobilization and inflammation. Endocrinology 151:2504—2514.

[77] Wang, R.H., Li, C., Deng, C.X., 2010. Liver steatosis and increased ChREBP expression in mice carrying a liver specific SIRT1 null mutation under a normal feeding condition. International Journal of Biological Sciences 6:682—690.

[78] Francque, S., Verrijken, A., Caron, S., Prawitt, J., Paumelle, R., Derudas, B., et al., 2015. PPARalpha gene expression correlates with severity and histological treatment response in patients with non-alcoholic steatohepatitis. Journal of Hepatology 63:164—173.

[79] Wu, T., Liu, Y.H., Fu, Y.C., Liu, X.M., Zhou, X.H., 2014. Direct evidence of sirtuin downregulation in the liver of non-alcoholic fatty liver disease patients. Annals of Clinical Laboratory Science 44:410—418.

[80] Auguet, T., Berlanga, A., Guiu-Jurado, E., Terra, X., Martinez, S., Aguilar, C., et al., 2014. Endocannabinoid receptors gene expression in morbidly obese women with nonalcoholic fatty liver disease. BioMed Research International, 502542.

[81] Gjorgjieva, M., Sobolewski, C., Dolicka, D., Correia de Sousa, M., Foti, M., 2019. miRNAs and NAFLD: from pathophysiology to therapy. Gut 68:2065—2079.

[82] Lopez-Riera, M., Conde, I., Quintas, G., Pedrola, L., Zaragoza, A., Perez-Rojas, J., et al., 2018. Non-invasive prediction of NAFLD severity: a comprehensive, independent validation of previously postulated serum microRNA biomarkers. Scientific Reports 8:10606.

[83] Hu, Y., Liu, H.X., Jena, P.K., Sheng, L., Ali, M.R., Wan, Y.Y., 2020. miR-22 inhibition reduces hepatic steatosis via FGF21 and FGFR1 induction. JHEP Rep 2:100093.

[84] Gurha, P., Wang, T., Larimore, A.H., Sassi, Y., Abreu-Goodger, C., Ramirez, M.O., et al., 2013. microRNA-22 promotes heart failure through coordinate suppression of PPAR/ERR-nuclear hormone receptor transcription. PloS One 8:e75882.

[85] Iliopoulos, D., Malizos, K.N., Oikonomou, P., Tsezou, A., 2008. Integrative microRNA and proteomic approaches identify novel osteoarthritis genes and their collaborative metabolic and inflammatory networks. PloS One 3:e3740.

[86] Chen, H., Lu, Q., Fei, X., Shen, L., Jiang, D., Dai, D., 2016. miR-22 inhibits the proliferation, motility, and invasion of human glioblastoma cells by directly targeting SIRT1. Tumour Biol 37:6761—6768.

[87] Zhang, X., Li, Y., Wang, D., Wei, X., 2017. miR-22 suppresses tumorigenesis and improves radiosensitivity of breast cancer cells by targeting Sirt1. Biological Research 50:27.

[88] Pant, K., Yadav, A.K., Gupta, P., Islam, R., Saraya, A., Venugopal, S.K., 2017. Butyrate induces ROS-mediated apoptosis by modulating miR-22/SIRT-1 pathway in hepatic cancer cells. Redox Biol 12:340—349.

[89] Tsuchiya, N., Izumiya, M., Ogata-Kawata, H., Okamoto, K., Fujiwara, Y., Nakai, M., et al., 2011. Tumor suppressor miR-22 determines p53-dependent cellular fate through post-transcriptional regulation of p21. Cancer Research 71:4628—4639.

[90] Panasiuk, A., Dzieciol, J., Panasiuk, B., Prokopowicz, D., 2006. Expression of p53, Bax and Bcl-2 proteins in hepatocytes in non-alcoholic fatty liver disease. World Journal of Gastroenterology 12:6198—6202.

[91] Yahagi, N., Shimano, H., Matsuzaka, T., Sekiya, M., Najima, Y., Okazaki, S., et al., 2004. p53 involvement in the pathogenesis of fatty liver disease. Journal of Biological Chemistry 279:20571—20575.

[92] Yan, Z., Miao, X., Zhang, B., Xie, J., 2018. p53 as a double-edged sword in the progression of non-alcoholic fatty liver disease. Life Sciences 215:64—72.

[93] Krstic, J., Galhuber, M., Schulz, T.J., Schupp, M., Prokesch, A., 2018. p53 as a dichotomous regulator of liver disease: the dose makes the medicine. International Journal of Molecular Sciences 19.

[94] Reed, S.M., Quelle, D.E., 2014. p53 acetylation: regulation and consequences. Cancers 7:30–69.

[95] Derdak, Z., Villegas, K.A., Harb, R., Wu, A.M., Sousa, A., Wands, J.R., 2013. Inhibition of p53 attenuates steatosis and liver injury in a mouse model of non-alcoholic fatty liver disease. Journal of Hepatology 58:785–791.

[96] Baffy, G., 2015. MicroRNAs in nonalcoholic fatty liver disease. Journal of Clinical Medicine 4:1977–1988.

[97] Chang, J., Davis-Dusenbery, B.N., Kashima, R., Jiang, X., Marathe, N., Sessa, R., et al., 2013. Acetylation of p53 stimulates miRNA processing and determines cell survival following genotoxic stress. The EMBO Journal 32:3192–3205.

